Tectonics®

RESEARCH ARTICLE
10.1029/2022TC007533

Key Points:

- Early middle Devonian positive εHf results evidence juvenile magmatic input in the western North Patagonian Massif
- Extensional to contractional tectonic switch was recognized during Devonian-early Carboniferous times in northwestern Patagonia
- Two segments in South America shows contrasting tectonic evolution with contractional and extensional coetaneous regimes

Supporting Information:

Supporting Information may be found in the online version of this article.

Correspondence to:

P. Marcos,
pmarcos@unrn.edu.ar;
paulomarcos89@hotmail.com

Citation:

Marcos, P., Renda, E. M., González, P. D., Oriolo, S., Scivetti, N., Benedini, L., et al. (2023). Devonian to early Carboniferous retreating—Advancing subduction switch in the northwestern Patagonia accretionary orogen: U-Pb and Lu-Hf isotopic insights. *Tectonics*, *42*, e2022TC007533. https://doi.org/10.1029/2022TC007533

Received 10 AUG 2022
Accepted 25 OCT 2023

Devonian to Early Carboniferous Retreating—Advancing Subduction Switch in the Northwestern Patagonia Accretionary Orogen: U-Pb and Lu-Hf Isotopic Insights

Paulo Marcos[1,2], Emiliano M. Renda[1,2], Pablo D. González[3], Sebastián Oriolo[4], Nicolás Scivetti[5], Leonardo Benedini[6,7], Mauro Geraldes[8], Daniel Gregori[6,7], María Belén Yoya[4], and Marcos Bahía[6,9]

[1]Universidad Nacional de Río Negro, Instituto de Investigación en Paleobiología y Geología, Río Negro, Argentina, [2]IIPG, UNRN, CONICET, General Roca, Argentina, [3]CONICET-SEGEMAR, Regional Sur, General Roca, Argentina, [4]CONICET-Universidad de Buenos Aires, Instituto de Geociencias Básicas, Aplicadas y Ambientales de Buenos Aires (IGEBA), Buenos Aires, Argentina, [5]Instituto Patagónico de Geología y Paleontología –IPGP- (CENPAT-CONICET), Puerto Madryn, Argentina, [6]Instituto Geológico del Sur (INGEOSUR), Universidad Nacional del Sur (UNS)-CONICET, Bahía Blanca, Argentina, [7]Departamento de Geología, Universidad Nacional del Sur (UNS), Bahía Blanca, Argentina, [8]Departamento de Geología Regional, Facultad de Geología, Universidad Estatal de Río de Janeiro, Rio do Janeiro, Brazil, [9]Departamento de Física, Universidad Nacional del Sur (UNS), Bahía Blanca, Argentina

Abstract In this contribution, we present new early middle Devonian igneous and metaigneous units with a major juvenile magmatic source input in the North Patagonian Massif, which were discovered through U-Pb and Lu-Hf zircon analyses. Afterward, we assessed their tectonic implications for northwestern Patagonia and then for southern South America, combining our results with available database information consisting of igneous crystallization ages and isotopic data of the Devonian to early Carboniferous magmatic units, tectonic-metamorphic analyses, and thermochronologic record. This study allows for distinguishing retreating and advancing subduction switching in northwestern Patagonia (38°30′ to 44°S) and a contrasting coetaneous evolution for basement outcrops exposed further north (27°30′ and 37°30′S). The early middle Devonian (400–380 Ma) northwestern Patagonian magmatism is characterized by widespread magmatism and positive εHf–εNd linked to forearc and backarc magmatism that evolved within a retreating subduction stage. A tectonic switching toward advancing orogeny stage began in the late Devonian, evidenced by a lull in magmatic activity with a negative εHf–εNd trend, possibly contemporaneous with the first tectonic-metamorphic event in western Patagonia. An early Carboniferous magmatic gap, followed by the subsequent development of the main foliation in the basement during the Carboniferous-Permian period, denotes the acme of this contractional stage. In contrast, the Devonian period in the northern segment is characterized by mostly negative εHf–εNd values, reverse shear zone activity in the foreland, and an inboard magmatism migration, evidencing a compressive tectonic setting that changed to an extensional configuration in the early Carboniferous with widespread arc magmatism development.

1. Introduction

The Gondwana supercontinent is composed of Precambrian cratons sutured by Neoproterozoic orogenic belts (Cawood & Buchan, 2007) and surrounded by Paleozoic orogenic systems along its continental margins. The Terra Australis Orogen (ca. 570 to 300 Ma) and the Gondwanide Orogen (ca. 300 to 250 Ma) documented the Paleozoic evolution from Gondwana amalgamation to Pangea assembly times (Cawood, 2005). The Paleozoic orogenic growth of southwestern Gondwana is one of the most debated subjects in southern South America, since contrasting paleotectonic scenarios of continent collision against accretionary orogens have been proposed for both orogenies in the last decades (e.g., Dahlquist et al., 2021; Forsythe, 1982; González et al., 2018; Hervé et al., 2016; Oriolo et al., 2021, 2023; Pankhurst et al., 2006; Ramos, 2008). In any case, the combination of the magmatic, metamorphic, and structural record, along with geochronologic/thermochronologic and isotopic data, is crucial for deciphering the nature of orogenic growth and defining how their contractional and extensional stages evolved over time and space.

The Devonian to early Carboniferous igneous rocks are distributed into two major regions in southern South America. The northern segment is restricted between 27°30′ and 37°30′S and encompasses the Coastal Cordillera,

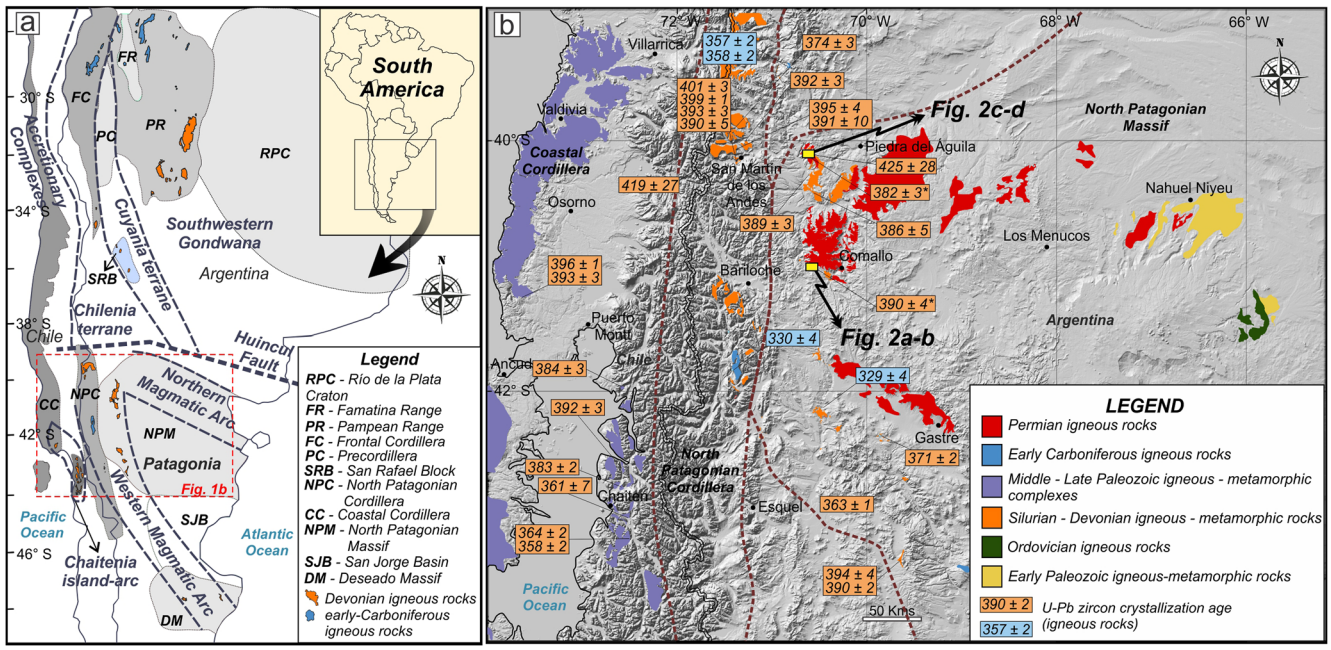

Figure 1. (a) Sketch map showing the Devonian—early Carboniferous igneous units in South America and its tectonostratigraphic regions and terrane blocks boundaries (compiled and modified from Hervé et al. (2016), Mosquera and Ramos (2006), Ramos (2008), Dahlquist et al. (2021), and Oriolo et al. (2023)). (b) Geologic sketch map showing the Paleozoic units of the north Patagonia (modified from Marcos et al. (2020)). Locations of study areas (Figures 2a and 2c) are shown by yellow-filled rectangles. The zircon crystallization ages of the Devonian - early Carboniferous igneous units follow the 2022 chronostratigraphic chart of Cohen et al. (2013) and the data are from: Duhart et al. (2001, 2009), Hervé et al. (2013, 2016, 2018), and Rapela et al. (2021) for the Coastal Cordillera; and Varela et al. (2005), Pankhurst et al. (2006), Serra-Varela et al. (2021), Rapela et al. (2021, 2022), Renda et al. (2022), and Oriolo et al. (2023), and this work (*) for North Patagonian Cordillera and North Patagonian Massif (Table S1 in Supporting Information S1).

Principal Cordillera, Frontal Cordillera, Precordillera, Famatina Range, Pampean Ranges, and San Rafael Block (Figure 1a), while the exposures of the southern segment are mainly distributed in the northwestern Patagonia region (38°30′ to 44°S). In the latter, the Devonian-early Carboniferous basement crops out in the Coastal Cordillera, North Patagonian Cordillera and the western part of the North Patagonian Massif (e.g., Oriolo et al., 2023), encompassing the northern part of the western magmatic arc proposed by Ramos (2008) (Figure 1a). In last years, the increase in the understanding of Devonian and Carboniferous magmatic processes in northwestern Patagonia has been mainly related to geologic, geochronologic, and isotopic contributions (e.g., Hervé et al., 2013; Oriolo et al., 2023; Pankhurst et al., 2006; Rapela et al., 2021). These contributions are, however, mainly restricted to the Coastal Cordillera and North Patagonian Cordillera, while the western North Patagonian Massif has not been widely explored, and thus, its geologic and geochronologic-isotopic records are unknown in many areas.

This contribution analyzes the igneous-metamorphic exposures located in two key areas of the western North Patagonian Massif (Figures 1c and 2), providing new U-Pb zircon crystallization ages and Lu-Hf isotopic analysis. The Devonian magmatic record of these units have geodynamics implications for the northwestern Patagonia region. Therefore, we combined our results with available P-T, thermochronologic, and structural data from coeval metamorphic rocks to evaluate and characterize how the contractional and extensional stages evolved. Subsequently, we propose a Devonian-early Carboniferous geotectonic model for northwestern Patagonia. Furthermore, we compare these stages with their counterparts in the northern segment, highlighting contrasting settings and along-strike segmentation of the southwestern Gondwana margin during Devonian—early Carboniferous times.

2. Geologic Setting

The igneous-metamorphic basement in northern Patagonia is distributed across the North Patagonian Massif, North Patagonian Cordillera, and Coastal Cordillera (Figure 1b). The Huincul Fault is an intracratonic strike-slip fault system that behaves as the subsurface northern basement boundary at approximately 38° S (Figure 1a;

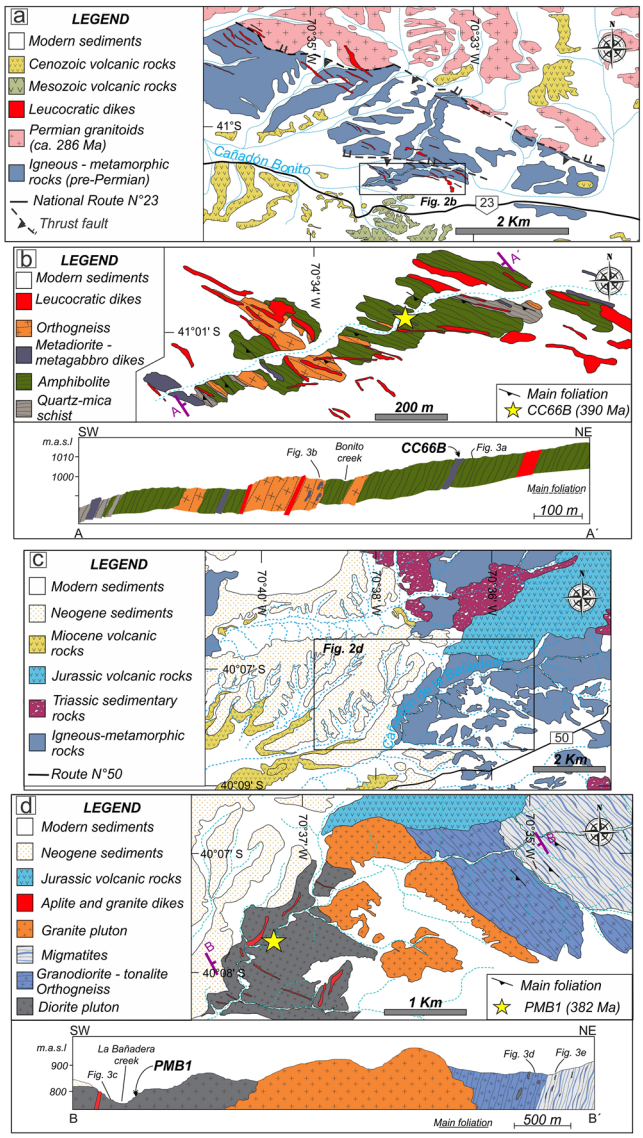

Figure 2. Geologic maps of Cañadón Bonito (a, b) and Cañadon de la Bañadera (c, d) in the western North Patagonian Massif. (a) Location of the study area showing the distribution of the Paleozoic basement and volcano-sedimentary rocks (modified from Marcos, 2020). (b) Detailed map and cross section of the Cañadon Bonito. (c) Location of the study area showing the distribution of the igneous-metamorphic basement and younger volcanic-sedimentary outcrops (modified from Escosteguy et al., 2013). (d) Detailed map and cross section of the Cañadon de La Bañadera. Locations of maps of (a, c) are shown in Figure 1b. Locations of samples of Figures 3a, 3b, and 3c–3e are inserted in profiles to (b, d), respectively.

e.g., Chernicoff & Zappettini, 2004; Mosquera & Ramos, 2006; Gregori et al., 2008). On the other hand, geophysical studies and borehole data (e.g., Renda et al., 2019) denote the continuity of the Patagonia western magmatic arc (Ramos, 2008) toward southeastern direction under the San Jorge Basin, which then crops out in the Deseado Massif (Figure 1a; Ramos & Naipauer, 2014). However, Devonian igneous geochronologic and isotopic data are scarce in the latter, and its outcrops are far away from the northern Patagonia (Figure 1a; Pankhurst et al., 2003; Ballivián Justiniano et al., 2023; de Barrio et al., 2023). Therefore, the regional study area of this work was limited to latitudes between 38°30′ and 44°S.

The early Cambrian metamorphic and igneous units of the eastern North Patagonian Massif are the oldest chronostratigraphic record in northern Patagonia (Greco et al., 2015, 2017; Pankhurst et al., 2006; Rapalini et al., 2013). Low to high-grade metamorphism was subsequently developed during late Cambrian-early Ordovician (González et al., 2018), whereas a syn- to post-orogenic middle Ordovician magmatic event took place afterward (Figure 1b; Pankhurst et al., 2006). The Cambrian to Ordovician tectonomagmatic record is mainly restricted to northeastern Patagonia (González et al., 2021).

The tectonomagmatic and metamorphic evolution shifted toward the southwest during Devonian-Carboniferous times, encompassing the western North Patagonian Massif, the North Patagonian Cordillera and several sectors of the Coastal Cordillera (Figure 1b; e.g., Varela et al., 2005; Marcos et al., 2018; Suárez et al., 2019, 2021). The oldest Devonian igneous rocks have crystallization ages close to 400 Ma and crop out in the North Patagonian Cordillera (Figure 1b; Pankhurst et al., 2006). Widespread magmatism developed subsequently (395–383 Ma), whereas minor igneous activity occurred close to the Devonian - Carboniferous limit (Oriolo et al., 2023).

The P-T and thermochronologic database reveals medium- to high-grade metamorphism primarily constrained from late Devonian to early Permian times (e.g., Duhart et al., 2001; Kato et al., 2008, 2009; Lucassen et al., 2004; Martin et al., 1999; Oriolo et al., 2019; Renda et al., 2021; Urraza et al., 2019; Willner et al., 2004). Exceptions were identified in the North Patagonian Cordillera, associated with Silurian migmatization (430 ± 5 Ma; Serra-Varela et al., 2019) and an early middle Devonian high-grade metamorphism (5 Kbar; 600°C) recorded in a migmatite paragneiss (392 ± 4 Ma; Martínez et al., 2012).

An earlier metamorphic stage, possibly developed in the late Devonian (Kato et al., 2008; Plissart et al., 2019; Renda et al., 2021), was subsequently overprinted by the NW-SE regional foliation during the Carboniferous and early Permian periods (Duhart et al., 2001; García-Sansegundo et al., 2009; Gregori et al., 2020; Marcos et al., 2020; Oriolo et al., 2019; Palape et al., 2022; Richter et al., 2007). The oldest metamorphic foliation is preserved as inclusions in porphyroblasts in certain areas of the North Patagonian Massif (e.g., López de Luchi et al., 2010), while late Devonian metamorphism has been documented in blueschists boulders (Kato et al., 2008) and suggested for ultramafic rocks (Plissart et al., 2019) in the Coastal Cordillera.

Afterward, the regional late Carboniferous - early Permian tectonometamorphic event associated with the main foliation of the basement reached amphibolite facies in many areas of the western North Patagonian Massif and the North Patagonian Cordillera, while greenschist-blueschist facies were developed in the Coastal Cordillera (Duhart et al., 2001; Marcos et al., 2020; Oriolo et al., 2019; Palape et al., 2022). However, it should be noted that several studies proposed that both the earlier and main foliations were developed exclusively during

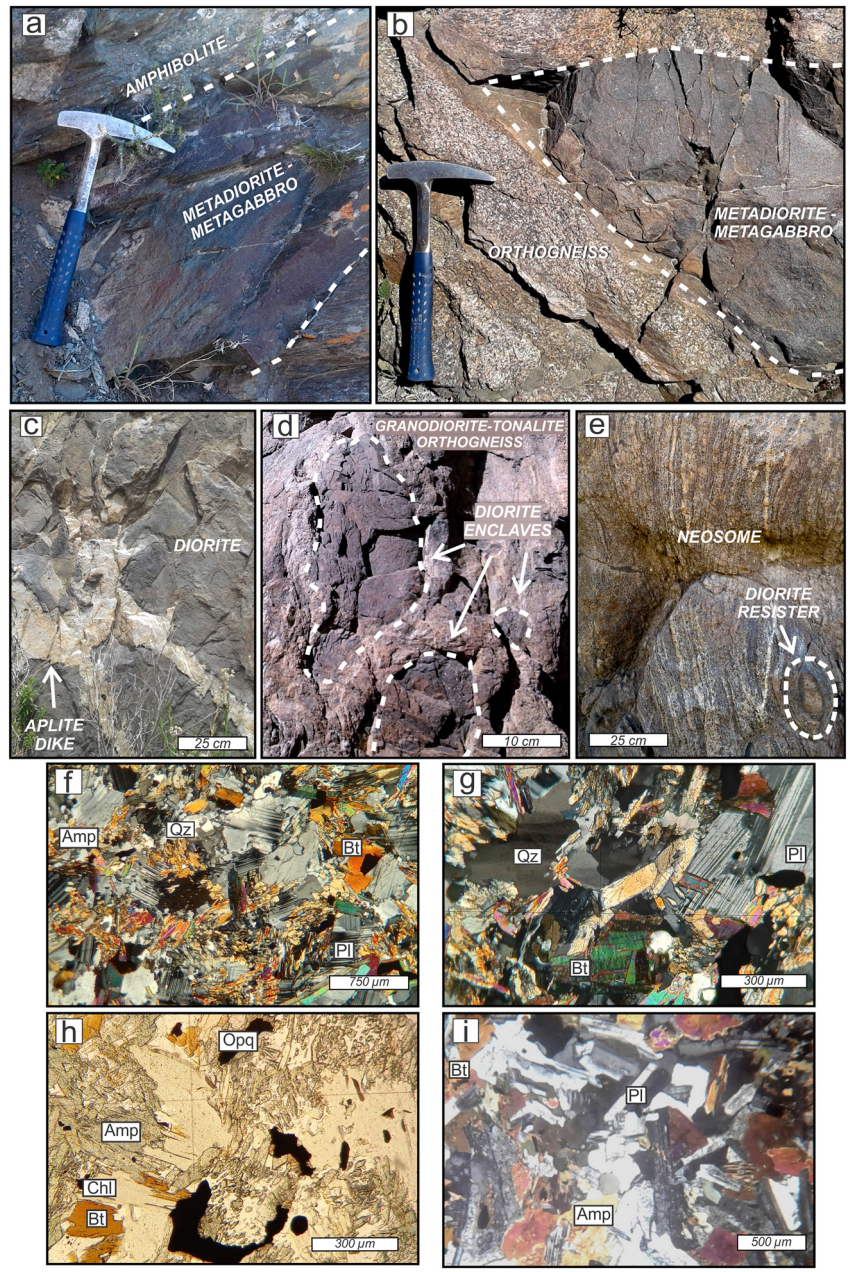

Figure 3. Images and photomicrographs of the basement in the Cañadón Bonito (a, b, f, g, h) and Cañadon de la Bañadera (c, d, e, i). (a) Metadiorite-metagabbro dike intrusion into the amphibolite unit. (b) Orthogneiss outcrop showing a metadiorite-metagabbro enclave. (c) Diorite pluton intruded by aplite dike. (d) Diorite enclave within tonalite-granodiorite orthogneiss. (e) Migmatite outcrop showing a diorite resister. (f–g) Crossed polarized photomicrographs of the diorite sample (CC66B) showing equigranular fine grain texture (f), deformation evidences like plagioclase twin migration and quartz subgrain boundary migration (g). (h) Polarized photomicrograph of the sample CC66B showing greenschist metamorphism overprint related to chlorite pseudomorphic replacement of clinoamphibole and biotite (h). (i) Crossed polarized photomicrograph of the diorite sample (PMB1) showing equigranular medium grain terxture. Locations of samples (a, b) and (c–e) are shown in profiles to Figures 2b and 2d, respectively. Mineral abbreviations follow Whitney and Evans (2010).

the Carboniferous-early Permian periods, as the result of progressive transpressional deformation (e.g., von Gosen, 2009; Oriolo et al., 2019; Palape et al., 2022). This last period marked the final stage of the Terra Australis Orogen and the beginning of the Gondwanide Orogen in western Patagonia after the early Carboniferous magmatic gap (Renda et al., 2021; Yoya et al., 2023).

3. Paleozoic Geotectonic Models

The Patagonian region has been interpreted in the context of contrasting Paleozoic geotectonic models that can be differentiated into allochthonous, parautochthonous and autochthonous with respect to southwestern Gondwana. In this section, we attempt to summarize the most contrasting models proposed for the north and western magmatic arcs of Patagonia, following the subdivision outlined by Ramos (2008).

An early collisional stage between East Antarctica and Patagonia (middle-late Cambrian; Ramos & Naipauer, 2014) followed by their collision against the southwestern Gondwana margin during the late Paleozoic has been proposed for the northern magmatic arc (e.g., Ramos, 1984; Ramos et al., 2020; Rapalini et al., 2010). Instead, González et al. (2018) proposed an early Paleozoic (Cambrian-Ordovician) accretion of Patagonia-Antarctica along southwestern Gondwana. On the other hand, Rapalini et al. (2013) suggested a possible continuation of the early Paleozoic record from the Pampean Ranges to the northeastern North Patagonian Massif, and then proposed an autochthonous origin for the Patagonia region.

The western magmatic arc comprises Devonian to Permian igneous and metamorphic rocks. Three main evolutionary models have been proposed for this region. The allochthonous continental collision reconstructions exhibit significant differences among different proposals. One collisional model suggests the southward extension of the Chilenia terrane and its Devonian collision with the Gondwana margin (Martínez et al., 2012), following northern exposures of this terrane in the Frontal Cordillera that record a collisional event with the Cuyania terrane (Precordillera), as indicated by several contributions (e.g., Boedo et al., 2016; Willner et al., 2011). Alternatively, a Carboniferous continental collision in the western belt of Patagonia resulting from the docking of the Deseado Massif against the North Patagonian Massif was proposed by Pankhurst et al. (2006). However, the extension of the basement into the San Jorge Basin and the Deseado Massif led to a redefinition of the Carboniferous suture position, suggesting the collision of the Antarctic Peninsula with Patagonia as the most probable tectonic scenario, as suggested by Ramos (2008).

On the other hand, an accretionary orogen configuration has been proposed for the western magmatic arc development. According to this hypothesis, some contributions proposed the accretion of the Chaitenia island arc to the southwestern Gondwana (e.g., Hervé et al., 2016; Quezada Pozo, 2015; Rojo et al., 2021), while others suggest that variations in the dynamics of subduction between the proto-Pacific and Gondwana plates were the main mechanisms that triggered the tectonometamorphic and magmatic processes in western Patagonia during the late Devonian to early Carboniferous times (e.g., Marcos et al., 2020; Oriolo et al., 2023).

4. Analytical Procedures

Key areas of poorly studied igneous-metamorphic basement of the North Patagonian Massif were selected, namely, Cañadón Bonito and Cañadón de la Bañadera (Figures 1b and 2). A metadiorite sample (CC66B) from the Cañadón Bonito area and a diorite sample (PMB1) from the Cañadón de la Bañadera region were collected for zircon U-Pb and Lu-Hf analysis. Both samples were crushed and milled using a jaw crusher and then heavy minerals were separated by heavy liquids before concentration by handpicking. The zircon grains were mounted in epoxy and polished until obtaining the zircon grains exposure. Afterward, cathodoluminescence images were obtained with a scanning electron microscope (SEM-Quanta 250). Mineral separation, and U-Pb and Lu-Hf analysis of zircons, were performed at the Laboratory of Geochronology and Radiogenic Isotopes (MultiLab) of the Universidade do Estado do Rio de Janeiro (UERJ—Brazil) (see Text S1 in Supporting Information S1 for more details).

The cathodoluminescence images show many zircons with oscillatory zoning patterns related to magmatic crystallization (Figures 4a and 5a; Corfu et al., 2003; Kemp et al., 2006). On the other hand, few zircons have resorption textures (e.g., patches and lobes), which are possibly linked to a late magmatic or metamorphic stage (Corfu et al., 2003; Hoskin & Black, 2000; Kinny & Maas, 2003). Considering these textures, resorption zones were avoided during measurement, in order to obtain the magmatic crystallization age and its isotopic signal (Figures 4 and 5). The Lu-Hf isotopes were measured only in zircon spots with concordant U-Pb age results, and the corresponding U-Pb age was used to obtain zircon depleted mantle and crustal Hf model ages (T_{DM} and T^{C}_{DM}) (Text S1, Tables S4, and S5 in Supporting Information S1).

5. Results

The study areas belong to the northwestern part of the North Patagonian Massif and are located near the boundary with the North Patagonian Cordillera (Figure 1b). The geologic knowledge of both areas is limited, and only the

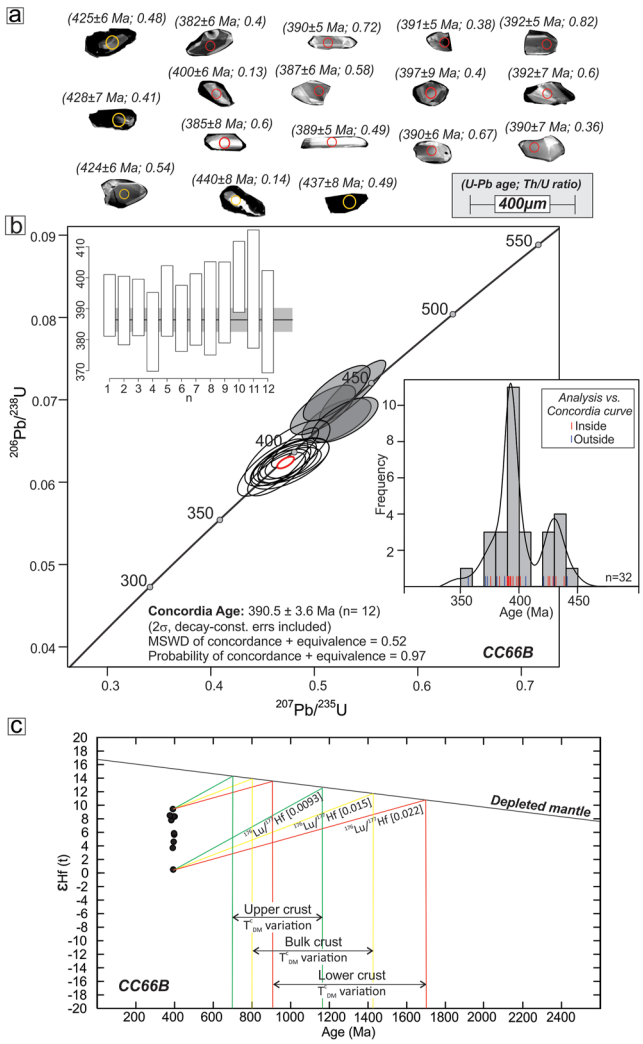

Figure 4. Cathodoluminescence image and zircon U-Pb ages and εHf isotopes results for sample CC66B belong to the metadiorite dike of Cañadón Bonito. (a) Cathodoluminescence image showing the zircons used to calculate the diorite crystallization age (red spots). The yellow spots show ages of inherited zircons. (b) Concordia diagram zircon U-Pb plots defining a crystallization age of 390.5 ± 3.8 Ma. Gray ellipses correspond to inherited zircon ages. The weighted mean of the 12 zircon ages that define the crystallization age is detailed in the upper-left diagram by a Gy bar. Frequency histogram made by analyses that plot inside (red lines) and outside (blue lines) to the Concordia curve is detailed in the lower right sector. (d) Plots of εHf(t) versus U-Pb zircon crystallization age. Note that zircon crustal model ages belong to different lower, upper and bulk crust Lu/Hf ratio estimations.

Cañadón de la Bañadera region has some geochronologic data that suggests a possible connection with the Devonian and Carboniferous magmatic arcs (Figure 1b; Varela et al., 2005; Rapela et al., 2022). Both areas could be linked to the northwestern part of the western magmatic arc proposed by Ramos (2008) and are situated inland with respect to the main outcrops of the Foreland Domain proposed by Rapela et al. (2021). However, we used only the names of each region (Coastal Cordillera, North Patagonian Cordillera, and western North Patagonian Massif) to refer to the location of any geologic, geochronologic, and/or isotopic information.

5.1. Cañadón Bonito

The Paleozoic basement crops out in creeks and low hills, and is covered by Mesozoic and Cenozoic volcanic-sedimentary deposits in surrounding areas near the Comallo locality (Figures 1b and 2a; Barros et al., 2020; Benedini et at. 2021, 2022). The Cañadón Bonito basement comprises quartz-mica schists, amphibolites, metadiorites-metagabbros dikes, orthogneisses, and leucocratic dikes (Figure 2b).

The biotite-quartz schists are scarce and develop lepidoblastic texture with a few plagioclase porphyroblasts. A foliated amphibolite is concordant with the quartz-mica schist, and shows lepidoblastic-nematoblastic (Bt, Chl, Amp, Ep) and granoblastic (Qz, Pl, Grt) bands. Metadiorite and metagabbro dikes intruded the quartz-mica schist and amphibolites (Figure 3a). These metaigneous dikes are equigranular fine-medium grain and have subhedral Pl + Amp ± Bt ± Cz ± Prh ± Qz ± Cal, and accessory minerals (Zrn, Rt, Ttn, Opq, Ap). Solid-state deformation and recrystallization evidence in these dikes is: (a) plagioclase twin boundary migration and quartz subgrain tiltwalls; (b) replacement of clinoamphibole and biotite by chlorite, and plagioclase by clinozoisite. Orthogneisses are medium-grained foliated rocks defined by granoblastic (Pl-Qz) and lepidoblastic (Bt-Chl-Grt-Ep) discontinuous bands, and have metadiorite-metagabbro enclaves (Figure 3b). In summary, the petrologic and structural features of all these lithofacies denote a greenschist - amphibolite facies metamorphism associated with a well-developed metamorphic foliation of 310°/65° SW. After this regional event, leucocratic dikes intrude mostly concordant to the main foliation (Figure 2b).

The CC66B sample belongs to the metaigneous dike unit and intrudes the foliated amphibolite in the middle section of the Cañadón Bonito (Figure 2b). This rock is an equigranular fine-grained metadiorite constituted by plagioclase (65%; An_{45-50}), clinoamphibole (30%), biotite (5%), opaque minerals (2%), quartz (~1%) and accessory minerals (Ap, Zr) (Figure 3f). Plagioclase twin migration, quartz subgrain boundaries migration (Figure 3g), and biotite and clinoamphibole pseudomorphic replacement by chlorite (Figure 3h), shows the solid-state and metamorphic overprint, respectively. This sample contains zircons crystals with size between 80 and 250 µm and elongation ratios (width/length) of 1:4 (9%), 1:3 (28%), 1:2 (52%), and 1:1 (11%). The elongated zircon groups are prismatic, euhedral to subhedral and have single or by-pyramidal development, while most of the shortest zircons develop subhedral and equidimensional crystals (Figure 4a). The results show Th/U ratios between 0.1 and 0.82, which are consistent with magmatic origin (Table S2 in Supporting Information S1; Rubatto, 2002), and individual U-Pb crystallization ages are between 438 and 340 Ma (Figure 4b). A few older zircon ages are discordant, whereas five concordant ages could be inherited xenocrysts (Figures 4a and 4b; Table S2 in Supporting Information S1). Most of the younger age groups yield imprecise U-Pb ages that might be linked to radiogenic Pb loss. Twelve concordant analyses were plotted on the Concordia diagram (Figure 4c and Table S2 in Supporting Information S1), indicating an early middle Devonian age of 390.5 ± 3.8 Ma (n = 12; MSWD = 0.52) for the zircon crystallization age of the metadiorite.

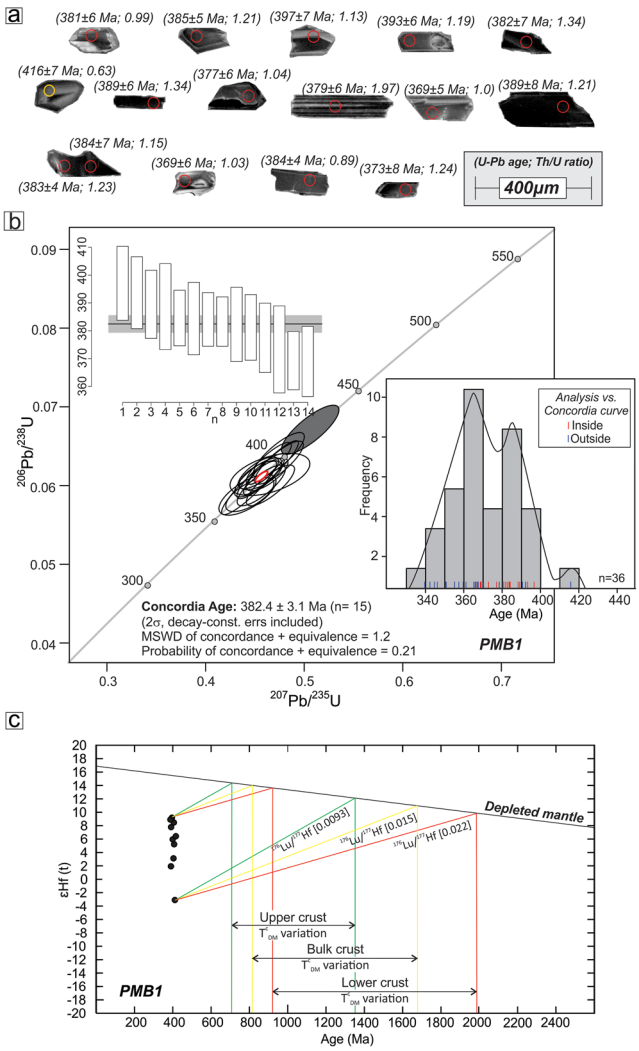

Figure 5. Cathodoluminescence image and zircon ages for diorite sample (PMB1) of Cañadón de la Bañadera. (a) Cathodoluminescence image showing the zircon used to calculate the diorite pluton crystallization age (red spots). The yellow spot shows the age of inherited zircon. (b) Concordia diagram zircon U-Pb plots defining a crystallization age of 382.4 ± 3.1 Ma. Gray ellipse corresponds to the inherited zircon. The weighted mean of the 15 zircon ages that define the crystallization age is detailed in the upper-left diagram by a Gy bar. Frequency histogram made by analyses that plot inside (red lines) and outside (blue lines) to the Concordia curve is also detailed. It is remarkable that most of the younger analysis plots outside the Concordia curve and produce a peak at ca. 360 Ma. (c) Plots of εHf(*t*) vs. U-Pb zircon crystallization age. Note that zircon crustal model ages belong to different lower, upper and bulk crust Lu/Hf ratio estimations.

The results of the Lu-Hf zircons composition of the metadiorite sample (CC66B) are summarized in Table S3 (Supporting Information S1). All the εHf(*t*) values are positive with an average of +6.3 and a variable range between +0.5 and + 9.4 (Figure 4c). The hafnium model ages (T_{DM}) are Precambrian, from 0.96 Ga to 0.61 Ga. On the other hand, zircon crustal model ages (T^c_{DM}) have a wide values range between 1.69 and 0.68 Ga. Considering the $^{176}Lu/^{177}Hf$ lower crust source composition, we obtained model ages (T^c_{DM}) between 1.69 and 0.9 Ga, whereas values from 1.17 Ga to 0.69 Ga were obtained by means of upper crust isotopic compositions. As could be expected, the crust bulk composition estimation yields intermediate crustal model ages with average values between 1.43 Ga and 0.8 Ga (Figure 4c; Tables S3 and S4 in Supporting Information S1).

5.2. Cañadón de la Bañadera

The igneous-metamorphic rock exposures are almost restricted to creeks and road tracks in the northwestern Patagonia region, since it is commonly covered by volcanic-sedimentary units (Figure 2c; Galli, 1969; Escosteguy et al., 2013; Dicaro et al., 2023). Plutons, dykes, and migmatites constitute the basement of Cañadón de la Bañadera (Figure 2d). Based on field relationships, it is possible to suggest the relative timing of intrusions of dioritic to granitic compositions. The diorite unit corresponds to the oldest stratigraphic igneous facies cropping out in the western region of the studied profile (Figures 2d and 3c). This facies forms medium- to fine-grained (0.8–2 mm) equigranular bodies, and is mainly made up of plagioclase, clinoamphibole and biotite. Zircon, apatite, titanite, and opaque minerals are present as accessory minerals. Orthogneiss and migmatite are transitional between each other in the northeastern study area. Both units have metamorphic foliation of 300°/75° SW and their contact with the diorite unit was not found. However, diorite enclaves in the orthogneiss (Figure 3d) and diorite resisters in the migmatite (Figure 3e) evidence that both units are younger. The orthogneiss unit has a poorly defined banded structure, while migmatites have diverse paleosome-neosome ratios and morphologies transitional between metatexite-diatexite groups following the classification of Sawyer and Brown (2008). A late granitic pluton crops out in the middle of the study area showing equigranular and porphyritic textures, while aplite and granitic dikes cross-cut the diorite facies (Figures 2d and 3c).

The PMB1 sample is an equigranular medium-grained diorite made up of plagioclase (55%; An_{50}), clinoamphibole (30%), biotite (15%) and accessory minerals (Opq, Ap, Zr and Rt), that was selected from the plutonic outcrop placed at the western Cañadón de la Bañadera region (Figure 2d). This sample contains zircons crystals with size between 100 and 450 µm and elongation ratios (width/length) of 1:4 (12%), 1:3 (56%), 1:2 (26%), and 1:1 (6%). The elongated zircon groups are primarily prismatic and subhedral, while a few of them preserve single- pyramid tips. The shortest zircons are subhedral and only a few develop equidimensional crystals (Figure 5a). The isotopes analyses yield Th-U ratios between 0.6 and 1.34, compatible with a magmatic origin (Table S2 in Supporting Information S1; Rubatto, 2002), and individual U-Pb concordia ages range calculations are between 416 and 342 Ma. The oldest concordant zircon could be inherited xenocrysts (Figures 5a and 5b; Table S2 in Supporting Information S1). Most of the younger groups yield discordant U-Pb ages that might be linked to radiogenic Pb loss. Fifteen analyses show a middle-upper Devonian magmatic crystallization age of 382.2 ± 3.1 Ma (n = 15; MSWD = 1.6) for the diorite sample (Figure 5b; Table S2 in Supporting Information S1).

The Lu-Hf zircon results of the Devonian diorite sample (PMB1) have an initial epsilon Hf average value of +5.42 and most values are positive with a range between +1.94 and + 9.2, except for one negative value (−3.08). The zircon model ages (T_{DM}) have a Mesoproterozoic to Neoproterozoic range from 1.1 Ga to 0.62 Ga, while the zircon crustal model ages (T^{c}_{DM}) yield a wider Precambrian interval. Considering the $^{176}Lu/^{177}Hf$ lower crust composition we obtained model ages (T^{c}_{DM}) between 2.0 Ga and 0.91 Ga. The crustal model ages have averages values between 1.36 Ga and 0.7 Ga considering upper crust isotopic ratios. On the other hand, intermediate crust bulk compositions yield average values between 1.64 Ga and 0.8 Ga (Figure 5c; Tables S3 and S5 in Supporting Information S1).

6. Discussion

6.1. The Devonian Magmatic Record in the Western North Patagonian Massif

At approximately 40°S, the Devonian magmatism is found mostly in the North Patagonian Cordillera, whereas records in the North Patagonian Massif are only documented further southeast at ∼ 42°S near to the Gastre locality (Figure 1b; Pankhurst et al., 2006). In this context, previous proposals indicated Devonian magmatism along a NNW-SSE-striking belt (e.g., Marcos et al., 2018; Rapela et al., 2021), which is further reinforced by geochronologic results in the Cañadón Bonito (∼41°S; Figure 1b). On the other hand, the middle Devonian diorite pluton in the Cañadón de la Bañadera shows a wider extension of the Devonian arc-related magmatism at 40°S (Rapela et al., 2021).

The Devonian metaigneous outcrops in Cañadón Bonito are one of the oldest igneous record of the North Patagonian Massif and contrast with the previously described granodioritic to granitic Permian plutons near the Comallo locality (Varela et al., 2005). The basement in Cañadón Bonito shows that the oldest chronostratigraphic stage is represented by schist and amphibolite units constrained to pre-middle Devonian times. Considering that the schists unit could has a sedimentary protolith, a maximum depositional age of ca. 440 Ma could be considered taking into account detrital zircon ages obtained in the western North Patagonian Massif (e.g., Dicaro et al., 2023; Hervé et al., 2018). The second stage is related to the emplacement of the early middle Devonian gabbro-diorite dikes (391 ± 4 Ma). Based on the structure of the orthogneiss and its field relationships, this unit could represent part of the Devonian magmatism stage previous to the emplacement of leucocratic dikes and Permian granitoids. This revised chronostratigraphic sequence challenges the interpretation of the results obtained by Marcos et al. (2020) a few kilometers southeast of the Cañadón Bonito. In this sense, the youngest zircon population age (∼369 Ma) of the metasedimentary sequences could belong to the first tectonometamorphic event. Nonetheless, it is also possible that the metamorphic basement shows a very heterogeneous record, with significant variations in P-T-D-t paths of different blocks located nearby, as documented in other regions of northern Patagonia (e.g., Martínez et al., 2012; Oriolo et al., 2019).

On the other hand, the diorite crystallization age of 382 ± 3 Ma in the Cañadón de la Bañadera is comparable with the U-Pb crystallization age of the granodioritic (389 ± 3; Rapela et al., 2022) and leucogranitic (386 ± 5; Varela et al., 2005) rocks placed at surrounding areas (Figures 1b and 2c). The subsequent tectono-magmatic events in Cañadón de La Bañadera followed by tonalite-granodiorite orthogneiss, migmatites and finally the emplacement of the granitic pluton and dikes are supported by field evidence (Figures 2d and 3c–3e). A late metamorphic overprint might have taken place at around ∼361 Ma based on zircon ages provided by Varela et al. (2005) and Rapela et al. (2022). In both localities (Cañadón Bonito and Cañadón de La Bañadera), the late Devonian metamorphic ages may record the oldest tectonic-metamorphic event (see Section 6.4).

6.2. Isotopic Record

The Lu-Hf and Sm-Nd isotopic systems allow assessing the magmatic source and the associated geodynamic setting through time (Collins et al., 2011; Scherer et al., 2007; Wang et al., 2009). The arrangement between the oceanic and continental plates through the subduction evolution defines the advancing and retreating stages of accretionary orogens (e.g., Cawood et al., 2011; Collins, 2002). Contractional settings are linked to advancing orogen stages, which ultimately result from enhanced interplate coupling and are likely to result from shallow or flat-slab subduction of oceanic lithosphere. In these settings, continental arc magmatism tends to record inboard migration patterns, magmatic gaps/lulls, and crustal shortening and thickening. In turn, the latter favors increasing crustal recycling processes that can be monitored by isotopic trends of igneous rocks toward negative εHf and

εNd values. In contrast, extensional regimes are linked to retreating orogen stages triggered by steeply dipping oceanic lithosphere subduction. In such a setting, continental arc magmatism record trenchwards migration, crustal thinning and a significant mantle-derived juvenile magmatic input that produces εHf and εNd positive signatures (e.g., Alasino et al., 2012; Collins et al., 2011; Du et al., 2021; Folguera & Ramos, 2011; Gianni et al., 2018; Kemp et al., 2009; Li et al., 2011; Nelson & Cottle, 2018; Oriolo et al., 2023; Wu et al., 2021). Throughout the subduction evolution, each regime can operate at different timescales, from ca. 10–30 My (Chapman et al., 2021).

In the North Patagonian Cordillera, the oldest tonalitic to granodioritic units (401 ± 3 to 390 ± 5 Ma) present relatively low εHf (*t*) values (+2.3 to −14) (Hervé et al., 2016; Rapela et al., 2021; Serra-Varela et al., 2021). In contrast, the Lu-Hf isotopic zircons results of both metadiorite (CC66B) and diorite (PMB1) samples show a mixed mantle-crust source for the magmatism in the North Patagonian Massif. This mixture is reflected by the following εHf pattern (Figures 4c and 5c): (a) Vertical appearance of εHf (*t*) values against U-Pb zircon ages (Scherer et al., 2007); (b) Within a single sample differences in εHf (*t*) values close to 10 units (Hawkesworth et al., 2010; Kemp et al., 2007); (c) All Hf-isotopic results plot below the depleted mantle curve (Kröner et al., 2014; Wang et al., 2009). Although it is necessary to employ more isotopic data, our results in the North Patagonian Massif show mainly positive εHf values inboard the continent at around 390 and 380 Ma at 40–41°S. In addition, these results are partially overlapped with those of the Coastal Cordillera and exhibit a relatively significant juvenile input recorded by the εHf and εNd versus U-Pb crystallization age diagram (Figure 6a). Based on these regional patterns, it is possible to suggest a progressive increment of mantle source participation through the early middle Devonian magmatism evolution in the northwestern Patagonia region resulting from widespread crustal extension, not only in the Coastal Cordillera but also in the northwestern section of North Patagonian Massif. Although suprachondritic or nearly chondritic εHf values persist until late Devonian times, the isotopic trend shows a negative trend from the middle to late Devonian periods, indicating a gradual transition toward more crustal compositions (Figure 6a).

6.3. Hafnium Model Ages

Though Lu-Hf and Sm-Nd isotopes have been proved as a sensitive tool to define mantle and crust contributions in magmatic sources and their tectonic significance (e.g., Belousova et al., 2006; Hawkesworth et al., 2019; Iizuka et al., 2005, 2017), the quantification of mantellic and crustal inputs is a difficult task, mainly due to multiple processes that may lead to the same bulk isotopic signal. For instance, the crustal contribution may arise from crustal anatexis or assimilation after the emplacement of a mantle-derived magma. In turn, the latter may have incorporated subducted sediments, which may modify its juvenile depleted signal (e.g., Nebel et al., 2011; Roberts & Spencer, 2015). Therefore, crustal model ages have to be considered only an approximation of the contribution of recycled continental crust, instead of an absolute crustal source age. In particular, some of the Devonian magmatic units show crustal recycling evidenced, for example, by the presence of inherited zircons (e.g., CC66B and PMB1 samples; Figures 4 and 5).

The lack of pre-Paleozoic crust outcrops in western Patagonia encourages us to assess the Hf model ages in detail. Therefore, we obtain Hf model ages employing different $^{176}Lu/^{177}Hf$ ratios (Amelin et al., 1999; Chauvel et al., 2014; Condie et al., 2011; Griffin et al., 2002; Pietranik et al., 2008) for Devonian magmatic samples (CC66B and PMB1; Tables S4 and S5 in Supporting Information S1), in order to avoid a bias induced by the selected $^{176}Lu/^{177}Hf$ ratio (e.g., bulk crust employed in most contributions). The Hf model age range obtained in this work is wider (Figures 4c and 5c) than previous model ages determined for the Devonian igneous northwestern Patagonian samples (Table S1 in Supporting Information S1). Therefore, these results denote a wide range of Hf model ages that could be considered as an age crust estimation of the underlying, reworked basement of Devonian magmatism.

The dominance of subchondritic compositions and Mesoproterozoic Hf model ages of North Patagonian Cordillera samples reinforce the significant role of recycled crust during Devonian magmatism, generally attributed to Mesoproterozoic lower crustal rocks (Rapela et al., 2021). There is, however, a general scatter of Paleo- to Mesoproterozoic model ages, that may point to the presence of a complex late Mesoproterozoic basement, comprising both metaigneous and metasedimentary rocks with variable isotopic compositions, that was significantly reworked during the middle-late Paleozoic (Oriolo et al., 2023). The latter is particularly evident by metasedimentary wall rocks of Devonian intrusions, that underwent assimilation and/or anatexis (Hervé et al., 2018; Serra-Varela et al., 2019). In contrast, suprachondritic compositions and younger Hf model ages obtained for the Coastal Cordillera samples denote a large input of juvenile Devonian mantle-derived magmatism (Rapela et al., 2021). Though previously reported Lu-Hf data in the North Patagonian Massif revealed isotopic compositions similar to those of the North Patagonian Cordillera (Rapela et al., 2021), samples CC66B and PMB1 also

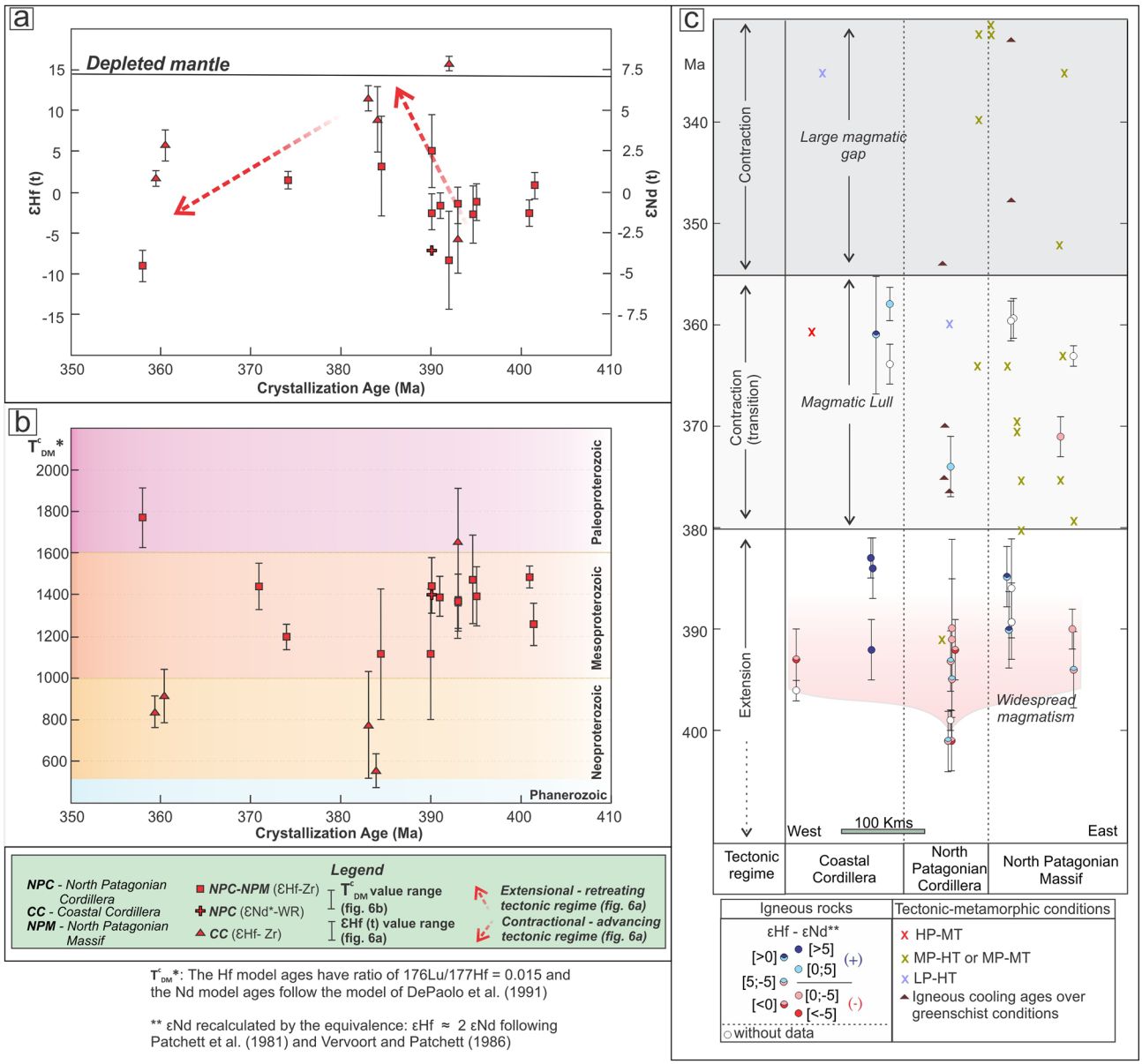

T^c_{DM}*: The Hf model ages have ratio of 176Lu/177Hf = 0.015 and the Nd model ages follow the model of DePaolo et al. (1991)

** εNd recalculated by the equivalence: εHf ≈ 2 εNd following Patchett et al. (1981) and Vervoort and Patchett (1986)

Figure 6. Devonian-early Carboniferous geochronologic and isotopic record of northwestern Patagonia. (a) Plots of εHf and εNd versus U-Pb zircon age showing positive isotopic trends during early middle Devonian (400-380 Ma) and negative during late Devonian times (ca. 380–360 Ma). (b) Bulk crustal model ages (T^c_{DM}) against U-Pb zircon ages showing primarily Mesopreterozoic crustal model ages for the NPC, NPM and Neoproterozoic for the CC. (c) Crystallization igneous ages against outcrops distribution within west-east relative distances. Widespread magmatism for the early middle Devonian times linked to extensional regime is distinguishable from the late Devonian magmatic lull and early Carboniferous magmatic gap belonging to a contractional regime. This contactional regime was coetaneous with HP-MT metamorphism in the CC and MP-HT metamorphism in the NPC and NPM. The metamorphism thermochronological data (Table S1 in Supporting Information S1) are from: Linares et al. (1988), Dalla Salda et al. (1991), Varela et al. (1991), Franzese (1995), Duhart et al. (2001), Ostera et al. (2001), Lucassen et al. (2004), Varela et al. (2005), Pankhurst et al. (2006), Kato et al. (2008), López de Luchi et al. (2010), Martínez et al. (2012), Urraza et al. (2019), Renda et al. (2021), González and Giacosa (2022), and Rapela et al. (2022).

show relatively juvenile contributions inboard and rather young Hf model ages with minor crustal reworking (Figure 6b).

6.4. Devonian to Early Carboniferous Tectonic-Magmatic Evolution in Northwestern Patagonia

Accretionary orogens along the southwestern Gondwana margin were simultaneously active with Eastern Gondwana counterparts during the Paleozoic development of the Terra Australis orogen (Cawood & Buchan, 2007).

The igneous-metamorphic basement of northwestern Patagonia shows a set of geologic features that might have evolved within advancing/contractional and retreating/extensional subduction tectonic settings during Devonian to early Carboniferous times. Crystallization ages against the orthogonal distance from the trench offers an interesting tool to analyze the oceanic-continental crust evolution through time and space (e.g., Gianni & Pérez, 2021). Nevertheless, choosing a confident arc-trench distance in an ancient Paleozoic arc setting, as in the case of northwestern Patagonia, is a challenge. To employ a suitable paleogeographic framework, we thus evaluated the time-space evolution of the Devonian-early Carboniferous magmatism considering west-east relative distances between igneous outcrops to avoid arc-trench distance estimations. On the other hand, the εHf–εNd evolutionary trends were employed to differentiate and characterize contractional and extensional regime stages (Section 6.2). Furthermore, a comprehensive analysis incorporating P-T conditions, thermochronologic ages and a compiled structural database was employed to define coeval tectonometamorphic events (Figure 6c). This integral analysis shows two major stages.

The oldest stage is constrained to early middle Devonian times (~400–380 Ma) and is likely characterized by an earlier normal subduction (ca. 400 Ma) that switched to a retreating subduction regime during the early middle Devonian (ca. 395–380 Ma). The earliest Devonian magmatism record in Patagonia belongs to tonalites of the North Patagonian Cordillera (401 ± 3 Ma; Pankhurst et al., 2006), which have an εHf range close to zero (Figures 1b, 6a, and 6c). Widespread magmatism encompassing several plutons distributed along ~75,000 Km^2 was subsequently developed (Figures 6c and 7a). This magmatic event (~395–380 Ma) has variable isotopic signatures that correspond to specific arc segments (Figure 7a). Most of the Coastal Cordillera samples have very positive εHf values that indicate magmatism in an extensional forearc (Rapela et al., 2021). The other segment with dominantly positive εHf values corresponds to the northwestern area of the North Patagonian Massif, possibly corresponding to a back-arc segment. In contrast, the continental arc axis likely extended from the North Patagonian Cordillera to the southwestern extreme of the North Patagonian Massif region (e.g., Rapela et al., 2021; Serra-Varela et al., 2021). This last segment has mostly negative εHf values and hence denotes a larger contribution of crustal recycling than the aforementioned areas. The isotopic signature of the early middle Devonian tectonic segments thus indicates an extensional/retreating orogen stage, where thinned continental crust and mantle upwelling in forearc and backarc areas were triggered by steeply proto-Pacific slab subduction from early to middle Devonian times (~395–380 Ma; Figure 7a).

The link between arc and back-arc magmatism and sedimentary record in northwestern Patagonia allow to consider at least two tectonic evolution scenarios. A Silurian passive margin sedimentation followed by an active continental margin evidenced by arc/back-arc Devonian magmatism is one possible tectonic evolutionary setting (e.g., Serra-Varela et al., 2020). On the other hand, the back-arc basin could be filled with sediments at an earlier stage (Silurian), and then was followed by Devonian arc/back arc magmatism developed within an extensional regime. This last model could explain the brief lapse of time between maximum depositation ages (~440 Ma) and the beginning of the Devonian magmatism (~400 Ma). Nonetheless, further data on metasedimentary rocks that constitute the wall-rocks of Devonian magmatism are required to evaluate these hypotheses.

The first evolutionary stage of our geodynamic model fits well with an extensional regime. The new results and the geodynamic reconstruction of the extensional regime contrast with the Chilenia continent collision model proposed for the early middle Devonian period (Martínez et al., 2012). Additionally, a difference between our model and that of Rapela et al. (2021) is related to a larger and more widespread lithospheric extensional setting. Previous proposals considered juvenile rocks of the coastal Cordillera as an evidence of the Chaitenia island arc (Hervé et al., 2016; Rapela et al., 2021). In this regard, our results indicate that the extensional stage not only affected the forearc but also the retroarc continental area, giving rise to juvenile back-arc magmatism as well, and thus enhancing the single subduction zone proposed recently by Oriolo et al. (2023) for the early middle Devonian.

The second stage is linked to a contractional regime that started by the late Devonian and progressed through late Paleozoic times (Figures 7b and 7c). A magmatic lull period could be distinguished for the very late Devonian stage, where igneous units developed a negative εHf trend with respect to the older igneous units (Figures 6a and 7b). This regional magmatic lull period might be linked to a rather shallow oceanic slab subduction setting (e.g., Gianni & Pérez, 2021; Zhang et al., 2019). In addition, this period is characterized by some thermochronologic records between 39° and 42°S which are linked to HP-MT eclogite-amphibolite metamorphism registered near to the paleo-trench in the Coastal Cordillera (Kato et al., 2008) and MP-MT/HT metamorphic

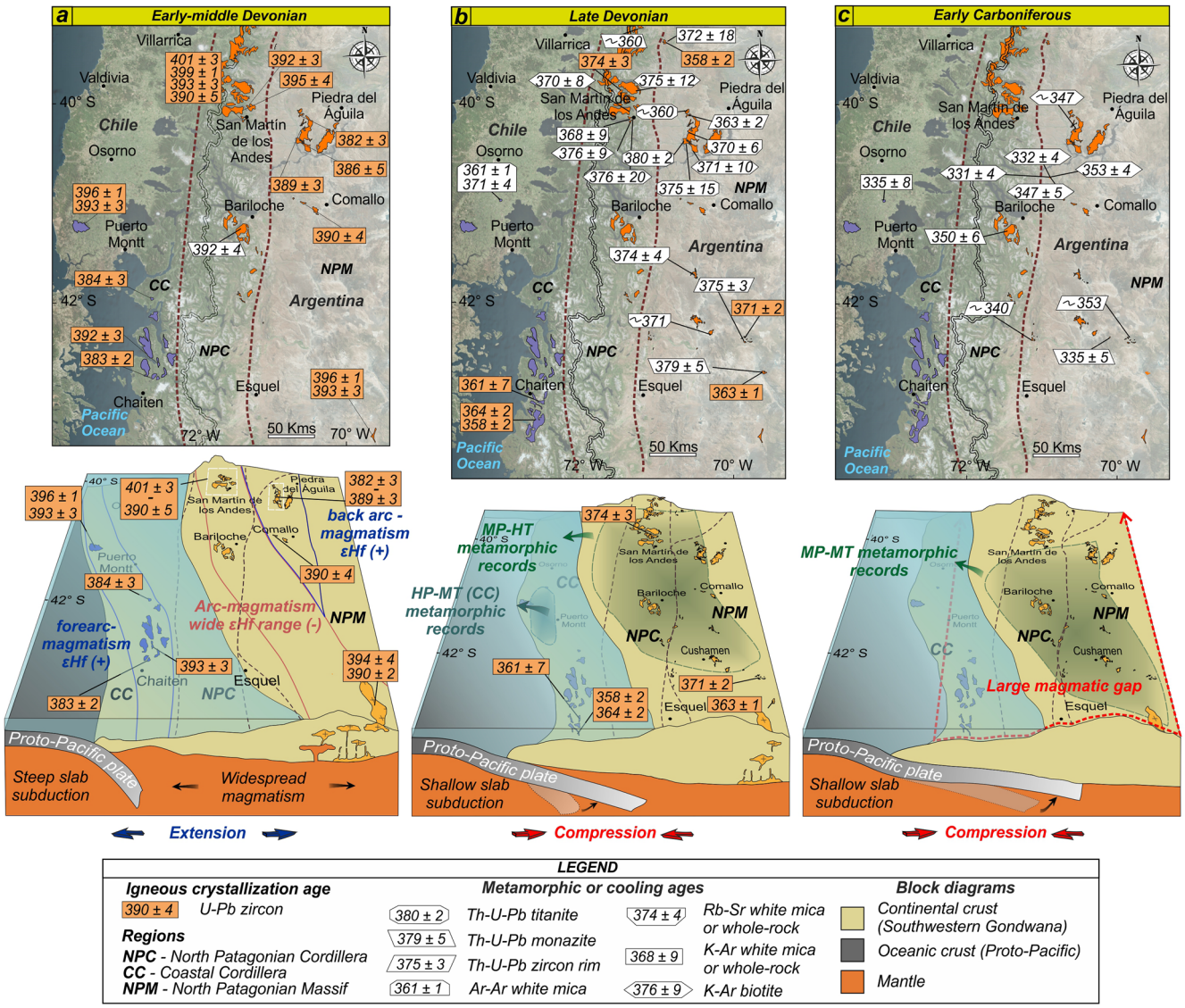

Figure 7. Sketch maps and block diagrams of the Devonian to early Carboniferous northwestern Patagonia geotectonic evolution. (a) Early middle Devonian widespread magmatism developed within extensional regime, where the forearc (CC) and backarc (northwestern part of the NPM) magmatism have positive εHf compared to the main arc encompassing the north part of NPC and southwest of the NPM. (b) Restricted magmatism production related to a regional magmatic lull coeval with the earliest thermochronological evidence of the late Devonian metamorphism. (c) Magmatic gap (~30 My) and the beginning of the regional metamorphism in northwestern Patagonia during the early Carboniferous.

conditions mainly recorded in the western North Patagonian Massif (Cerredo, 1997; Lucassen et al., 2004; Renda et al., 2021). This event could tentatively be the first tectonic-metamorphic event linked to an earlier foliation preserved as inclusion in porphyroblasts in the North Patagonian Cordillera and North Patagonian Massif (e.g., López de Luchi et al., 2010). However, further detailed petrochronologic studies are necessary to constrain the timing of this first tectonic-metamorphic event. Considering all these evolutionary patterns, it is possible to suggest a gradual tectonic switch from a retreating (early middle Devonian) to the beginning of an advancing regime (late Devonian) (Figures 7a and 7b). This earlier timing of the contractional stage contrasts with models that constrained the advancing orogen or collisional setting only after the late Devonian (e.g., Marcos et al., 2020; Oriolo et al., 2023; Pankhurst et al., 2006).

The early Carboniferous stage comprises a large magmatic gap in northwestern Patagonia (~30 My) that was subsequently interrupted by the protracted Gondwanide magmatism (~335–250 Ma; Oriolo et al., 2023) together with regional high- to medium-grade metamorphism and NW-SE metamorphic fabric development (e.g., Duhart

et al., 2001; Hervé et al., 1990; Marcos et al., 2020). This geodynamic framework of the second stage suggests a protracted contractional regime that progressed since the late Devonian and reached its peak during late Carboniferous to early Permian times (Figures 7b and 7c).

Although the development and subsequent accretion of the Chaitenia island-arc (Hervé et al., 2016; Rapela et al., 2021; Figure 1a) may represent the Devonian to early- Carboniferous geodynamic evolution, our results and analysis indicate that changes from extensional to contractional regime could be explained by steepness variations of the subducted slab (Figure 7). This model is closely related to recent geodynamic reconstruction for the late Paleozoic (e.g., Falco et al., 2022; Marcos et al., 2020; Oriolo et al., 2019, 2023). In this configuration, the presence of contemporaneous, paired metamorphic belts, with high-pressure metamorphism prevailing in the forearc and regional high-temperature metamorphism developing in the arc and back-arc region, documents the typical metamorphic architecture of an accretionary orogen (Brown, 2006, 2009).

6.5. Contrasting Devonian—Early Carboniferous Tectonic Setting in Southern South America

The Devonian-early Carboniferous magmatic rocks crop out not only in the Patagonia region but also further the northern basement areas of the southern South America (Figure 1a). In this work, we refer to the area between 27°30´ and 37°30´ S as the northern segment, which groups all of the Devonian-early Carboniferous magmatic rocks in the Coastal Cordillera, Principal Cordillera, Frontal Cordillera, Precordillera, Famatina Range, Pampean Ranges, and San Rafael Block. Diverse Paleozoic geotectonic models propose the presence of allochthonous-parautochthonous terranes named Cuyania (Ramos et al., 1986) and Chilenia (e.g., Boedo et al., 2016; Willner et al., 2023) encompassing the central-eastern region of the northern segment, while the basement placed at the western edge was named as Accretionary Complex (e.g., Hyppolito et al., 2014; Willner et al., 2004) (Figures 1a and 8). The geochronologic and isotopic record (Table S1 in Supporting Information S1), together with the tectonic-metamorphic, and thermochronologic data (Table S6 in Supporting Information S1) of the northern segment, denote a contrasting Devonian-early Carboniferous evolution respect to northwestern Patagonia.

A few negative εHf values (−16 to −5.4) and εNd close to zero (−6 to 0.1) in the early Devonian (413 ± 2 to 401 ± 4 Ma) magmatic rocks of the Frontal Cordillera and San Rafael Block may be linked to mixing of a mantle source with a recycled crustal component (Table S1 in Supporting Information S1; Dahlquist et al., 2020; Cingolani et al., 2017). The closure of the Neoproterozoic-Cambrian basin filled by sediments and volcanic-subvolcanic basic rocks belonging to the Guarguaraz Complex was contemporaneous with this active continental arc magmatism (López & Gregori, 2004) and triggered a high-pressure metamorphism in the Frontal Cordillera (Massonne & Calderón, 2008; Willner et al., 2011). The Devonian crustal shortening and thickening processes were associated with reverse shearing along older, reactivated shear zones and low-medium grade metamorphism in the Pampean Ranges (e.g., Garber et al., 2014; Ramos et al., 1998; Steenken et al., 2010). These tectonomagmatic and metamorphic patterns are compatible with a contractional tectonic regime (Figures 8a and 8b).

There are contrasting proposal regarding the geodynamic mechanism responsible of this contractional stage. The geologic record allows to consider a continental collision at 390 Ma of the Chilenia terrane (Frontal Cordillera) against the Cuyania terrane (Precordillera) (Boedo et al., 2021; Willner et al., 2011) and then an accretionary orogen evolution during the late Paleozoic (Willner et al., 2005, 2008, 2011). However, alternative tectonic reconstructions propose that Devonian - early Carboniferous period evolved within an accretionary orogeny, where tectonomagmatic and metamorphic evolution were linked to an advancing stage (Dahlquist et al., 2021; López & Gregori, 2004). Although the tectonic evolution is still a subject of debate and out of the scope of this contribution, evidence of a contractional regional setting during the Devonian period seems to be out of discussion.

The contractional setting of the northern segment contrasts with the extensional tectonic regime that prevailed in northwestern Patagonia during the early middle Devonian period (Section 6.4). This opposing behavior is possibly related to an along-strike segmentation of the margin, in line with previous proposals (e.g., Heredia et al., 2016; Hervé et al., 2016), where the contractional setting in the northern segment could be triggered by Chilenia terrane collision (e.g., Willner et al., 2011) or shallow subduction (e.g., Dahlquist et al., 2021). In contrast, the extensional/retreating regime in northwestern Patagonia was controlled by steep subduction (Figure 8a). A transitional late Devonian stage is characterized by the beginning of a contractional regime in northwestern Patagonia and a contractional regime ending in part of the northern segment which is linked to an inboard magmatism migration toward the Pampean Ranges (Dahlquist et al., 2021) (Figure 8b).

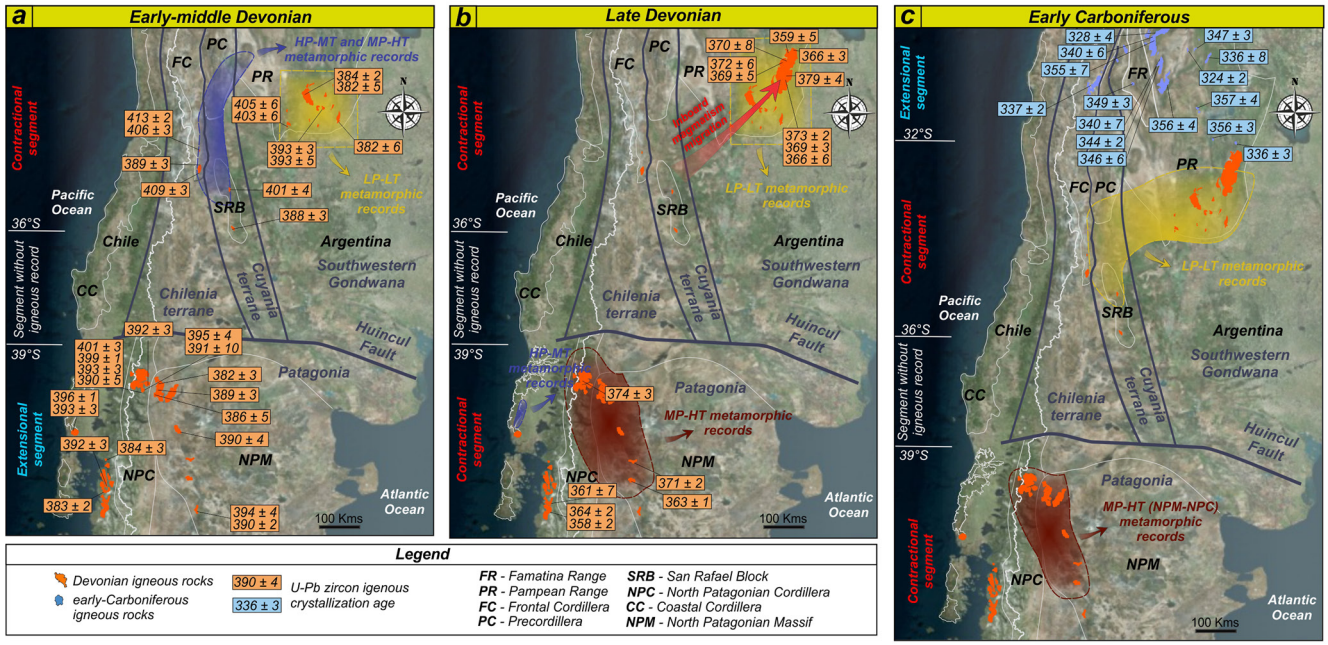

Figure 8. Sketch maps showing strike-segmented Devonian to early Carboniferous contrasting evolutions in southern South America. (a) Early middle Devonian extensional stage in northwestern Patagonia contrast with the contractional stage in the northern segment triggered by the Chilenia terrane collision or an advancing orogen regime. (b) Transitional late Devonian stage where inboard magmatism migration in the northern segment and earliest tectonic-metamorphic event in northwestern Patagonia denotes a contractional regime. (c) The early Carboniferous magmatism denotes a switch from contractional (Devonian) to extensional regime (early Carboniferous) in the north section of the northern segment (28°–32°S), while the southern section continued within a contractional setting. The zircon crystallization ages of the Devonian—early Carboniferous igneous units of the northern segment are from: Dorais et al. (1997), Stuart-Smith et al. (1999), Cingolani et al. (2003, 2017), Siegesmund et al. (2004), Rapela et al. (2008), Alasino et al. (2012, 2017), Dahlquist et al. (2013, 2014, 2019, 2020, 2021), Tickyj et al. (2015, 2017), Morosini et al. (2017), López de Luchi et al. (2017), Morales Cámera et al. (2018, 2020).

The early Carboniferous period also shows contrasting configurations between the northern segment and northwestern Patagonia. In northwestern Patagonia, the main stage of advancing regime is likely related to a shallower oceanic subduction slab (Figures 7c and 8c), which triggered the early- Carboniferous magmatic gap (Renda et al., 2021). On the other hand, the northern segment exhibits a latitudinal segmentation (Figure 8c). A widespread early Carboniferous magmatic episode with positive εNd trend is likely associated with an extensional setting recorded between 28° and 32°S (Figure 8c; Alasino et al., 2012). In contrast, the section between 32° and 35°S is characterized by the absence of magmatic records, basement exhumation, and reverse brittle-ductile shear zones in the Pampean Range, Frontal Cordillera and San Rafael Block (e.g., Bense et al., 2014, 2017; Löbens et al., 2017). Additionally, early Carboniferous high-pressure metamorphism developed in the Coastal Cordillera close to 34°S (Hyppolito et al., 2014). These geologic features from 32° to 35° south latitude allow to suggest a contractional regime for this area (Figure 8c).

7. Conclusion

New U-Pb and Lu-Hf zircons analyses in diorite igneous and metaigneous samples of the western North Patagonian Massif denotes juvenile input and subordinate crustal recycling in magmatic sources of rocks yielding crystallization ages of ca. 390–380 Ma. Taking into account contemporaneous igneous rocks in the North Patagonian Cordillera and Coastal Cordillera, results show a thinned continental crust linked to a retreating accretionary orogen. Furthermore, they suggest that the extensional lithospheric process was not restricted only to the Coastal Cordillera, as previously suggested, but also occurred in the back-arc region during the Lower to Middle Devonian (390–380 Ma).

An integrated analysis of the geochronologic, isotopic, P-T, thermochronologic, and structural data of the northwestern Patagonia basement allows differentiation of two stages with contrasting tectonic configurations in the accretionary orogen. During the early middle Devonian, an extensional/retreating regime was mainly evidenced by widespread magmatism occurring between 395 and 380 Ma and a positive trend in εHf-εNd values linked to

mantle upwelling in the forearc and back-arc. Subsequently, a period of reduced magmatic activity and a negative trend in εHf-εNd values likely indicate a distinct tectonometamorphic event, which may have marked the transition from a retreating to an advancing subduction orogen by the late Devonian. This contractional regime reached its peak during the Carboniferous to Lower Permian.

In southern South America, Devonian to early Carboniferous magmatic rocks crop out not only in the Patagonian region but also within a northern segment between 27°30′ and 37°30′S. The basement geologic record of the northern segment shows major discrepancies in tectonic regime compared to those of northwestern Patagonia. In this sense, the Devonian period is characterized by a contractional regime linked to the collision of the Chilenia terrane against the Gondwana margin (Willner et al., 2011) or an advancing orogen (Dahlquist et al., 2021) in the northern segment, thus contrasting with northwestern Patagonia, where an extensional retreating orogen prevails during the early middle Devonian. The second stage corresponds to the early Carboniferous, which exhibits an extensional configuration in the northern outcrops of the northern segment, while contractional setting in the Patagonia region triggered by shallow subduction.

Data Availability Statement

All data and software used in the manuscript are available in the text, figures, and Supporting Information S1 (Text S1 and Tables S1–S6) and can be found at https://data.mendeley.com/.

Acknowledgments
We would like to thank the people from the Comallo and Collón Curá region that allowed us access to their lands. We also thank to Dr. Taylor Schildgen, Editor in chief, and Dr. Augusto Rapalini, Associate Editor. We warmly acknowledge Martínez Dopico and two anonymous reviewers for their critical comments, which improved greatly the original manuscript. This contribution was supported by Grants PIP 11220200101662CO Consejo Nacional de Investigaciones Científicas y Técnicas (CONICET), PI- UNRN-2021-40-A-959 and PI-JI UNRN-2022-40-A-1095 Universidad Nacional de Río Negro.

References

Alasino, P. H., Dahlquist, J. A., Pankhurst, R. J., Galindo, C., Casquet, C., Rapela, C. W., et al. (2012). Early Carboniferous sub- to mid-alkaline magmatism in the eastern Sierras Pampeanas NW Argentina: A record of crustal growth by the incorporation of mantle-derived material in an extensional setting [Dataset]. Gondwana Research, *22*, 992–1008. https://doi.org/10.1016/j.gr.2011.12.011

Alasino, P. H., Larrovere, M. A., Rocher, S., Dahlquist, J. A., Basei, M. A. S., Memeti, V., et al. (2017). Incremental growth of an upper crustal, A-type pluton, Argentina: Evidence of a reused magma pathway [Dataset]. Lithos, *284–285*, 347–366. https://doi.org/10.1016/j.lithos.2017.04.013

Amelin, Y., Lee, D. C., Halliday, A. N., & Pidgeon, R. T. (1999). Nature of the Earth's earliest crust from hafnium isotopes in single detrital zircons [Dataset]. Nature, *399*(6733), 252–255. https://doi.org/10.1038/20426

Ballivián Justiniano, C. A. B., Oriolo, S., & Basei, M. A. (2023). Coupled U–Pb and Lu–Hf zircon data of late Devonian magmatism from bajo de La leona (deseado massif, Argentina): Tracking the southernmost exposure of the Devonian magmatic arc of Patagonia. *Journal of South American Earth Sciences*, *128*, 104455. https://doi.org/10.1016/j.jsames.2023.104455

Barros, M., Gregori, D., Benedini, L., Marcos, P., Strazzere, L., Pavon Pivetta, C., & Geraldes, M. (2020). Evolution of the Jurassic Comallo volcanic sedimentary complex in the western North Patagonian Massif, Rio Negro province, Argentina. *International Geology Review*, *63*(7), 1–23. https://doi.org/10.1080/00206814.2020.1731854

Belousova, E. A., Griffin, W. L., & O'Reilly, S. (2006). Zircon crystal morphology, trace element signatures and Hf isotope composition as a tool for petrogenetic modelling: Examples from Eastern Australian granitoids. *Journal of Petrology*, *47*(2), 329–353. https://doi.org/10.1093/petrology/egi077

Benedini, L., Barros, M., Pivetta, C. P., Stremel, A., Gregori, D. A., Marcos, P., et al. (2022). New insights into the Jurassic polyphase strain partition on the patagonian back-arc; constraints from structural analysis of ancient volcanic structures. *Tectonophysics*, *836*, 229430. https://doi.org/10.1016/j.tecto.2022.229430

Benedini, L., Pivetta, C. P., Marcos, P., Gregori, D. A., Barros, M., Scivetti, N., et al. (2021). Lower Jurassic felsic diatreme volcanism recognized in central Patagonia as evidence of along-strike rift segmentation. *Journal of South American Earth Sciences*, *106*, 102705. https://doi.org/10.1016/j.jsames.2020.102705

Bense, F., Costa, C., Oriolo, S., Löbens, S., Dunkl, I., Wemmer, K., & Siegesmund, S. (2017). Exhumation history and landscape evolution of the Sierra de San Luis (Sierras Pampeanas, Argentina)-new insights from low-temperature thermochronological data. *Andean Geology*, *44*(3), 275. https://doi.org/10.5027/andgeoV44n3-a03

Bense, F. A., Wemmer, K., Löbens, S., & Siegesmund, S. (2014). Fault gouge analyses: K–Ar illite dating, clay mineralogy and tectonic significance—A study from the Sierras Pampeanas, Argentina [Dataset]. International Journal of Earth Sciences, *103*(1), 189–218. https://doi.org/10.1007/s00531-013-0956-7

Boedo, F. L., Luján, S. P., Ariza, J. P., & Vujovich, G. I. (2021). The mafic-ultramafic belt of the Argentine Precordillera: A geological synthesis. *Journal of South American Earth Sciences*, *110*, 103354. https://doi.org/10.1016/j.jsames.2021.103354

Boedo, F. L., Willner, A. P., Vujovich, G. I., & Massonne, H. J. (2016). High-pressure/low-temperature metamorphism in the collision zone between the Chilenia and Cuyania microcontinents (western Precordillera, Argentina). *Journal of South American Earth Sciences*, *72*, 227–240. https://doi.org/10.1016/j.jsames.2016.09.009

Brown, M. (2006). Duality of thermal regimes is the distinctive characteristic of plate tectonics since the Neoarchean. *Geology*, *34*(11), 961–964. https://doi.org/10.1130/G22853A.1

Brown, M. (2009). Metamorphic patterns in orogenic systems and the geological record. *Geological Society, London, Special Publications*, *318*(1), 37–74. https://doi.org/10.1144/SP318.2

Cawood, P. A. (2005). Terra Australis Orogen: Rodinia breakup and development of the Pacific and Iapetus margins of Gondwana during the Neoproterozoic and Paleozoic. *Earth-Science Reviews*, *69*(3–4), 249–279. https://doi.org/10.1016/j.earscirev.2004.09.001

Cawood, P. A., & Buchan, C. (2007). Linking accretionary orogenesis with supercontinent assembly. *Earth-Science Reviews*, *82*(3–4), 217–256. https://doi.org/10.1016/j.earscirev.2007.03.003

Cawood, P. A., Leitch, E. C., Merle, R. E., & Nemchin, A. A. (2011). Orogenesis without collision: Stabilizing the Terra Australis accretionary orogen, eastern Australia. *Bulletin*, *123*(11–12), 2240–2255. https://doi.org/10.1130/B30415.1

Cerredo, M. E. (1997). The metamorphism of Cushamen formation, Río Chico area. North Patagonian Massif, Argentina. In *8th Congreso Geológico Chileno, Antofagasta, Actas* (Vol. 2, pp. 1236–1240).

Chapman, J. B., Shields, J. E., Ducea, M. N., Paterson, S. R., Attia, S., & Ardill, K. E. (2021). The causes of continental arc flare ups and drivers of episodic magmatic activity in Cordilleran orogenic systems. *Lithos*, *398*, 106307. https://doi.org/10.1016/j.lithos.2021.106307

Chauvel, C., Garçon, M., Bureau, S., Besnault, A., Jahn, B. M., & Ding, Z. (2014). Constraints from loess on the Hf–Nd isotopic composition of the upper continental crust [Dataset]. Earth and Planetary Science Letters, *388*, 48–58. https://doi.org/10.1016/j.epsl.2013.11.045

Chernicoff, C. J., & Zappettini, E. O. (2004). Geophysical evidence for terrane boundaries in south-central Argentina. *Gondwana Research*, *7*(4), 1105–1116. https://doi.org/10.1016/S1342-937X(05)71087-X

Cingolani, C. A., Basei, M. A. S., Llambias, E. J., Varela, R., Chemale Júnior, F., & Siga Júnior, O. (2003). The Rodeo Bordalesa tonalite, San Rafael block (Argentina): Geochemical and isotopic age constraints [Dataset]. Acta. https://doi.org/10.1007/978-3-319-50153-6_12

Cingolani, C. A., Llambías, E. J., Basei, M. A., Uriz, N. J., Chemale, F., & Abre, P. (2017). The Rodeo de la Bordalesa Tonalite dykes as a lower Devonian magmatic event: Geochemical and isotopic age constraints [Dataset]. In Pre-carboniferous evolution of the San Rafael block, Argentina (pp. 221–238). Springer. https://doi.org/10.1007/978-3-319-50153-6_12

Cohen, K. M., Finney, S. C., Gibbard, P. L., & Fan, J. X. (2013). The ICS international chronostratigraphic chart. *Episodes Journal of International Geoscience*, *36*(3), 199–204. https://doi.org/10.18814/epiiugs/2013/v36i3/002

Collins, W. J. (2002). Hot orogens, tectonic switching, and creation of continental crust. *Geology*, *30*(6), 535–538. https://doi.org/10.1130/0091-7613(2002)030<0535:HOTSAC>2.0.CO;2

Collins, W. J., Belousova, E. A., Kemp, A. I., & Murphy, J. B. (2011). Two contrasting Phanerozoic orogenic systems revealed by hafnium isotope data. *Nature Geoscience*, *4*(5), 333–337. https://doi.org/10.1038/ngeo1127

Condie, K. C., Bickford, M. E., Aster, R. C., Belousova, E., & Scholl, D. W. (2011). Episodic zircon ages, Hf isotopic composition, and the preservation rate of continental crust [Dataset]. Bulletin, *123*(5–6), 951–957. https://doi.org/10.1130/B30344.1

Corfu, F., Hanchar, J. M., Hoskin, P. W., & Kinny, P. (2003). Atlas of zircon textures. *Reviews in Mineralogy and Geochemistry*, *53*(1), 469–500. https://doi.org/10.2113/0530469

Dahlquist, J. A., Alasino, P. H., & Bello, C. (2014). Devonian F-rich peraluminous A-type magmatism in the proto-Andean foreland (Sierras Pampeanas, Argentina): Geochemical constraints and petrogenesis from the western-central region of the Achala batholith [Dataset]. Mineralogy and Petrology, *108*(3), 391–417. https://doi.org/10.1007/s00710-013-0308-0

Dahlquist, J. A., Cámera, M. M., Alasino, P. H., Pankhurst, R. J., Basei, M. A., Rapela, C. W., et al. (2021). A review of Devonian–Carboniferous magmatism in the central region of Argentina, pre-Andean margin of SW Gondwana [Dataset]. Earth-Science Reviews, *221*, 103781. https://doi.org/10.1016/j.earscirev.2021.103781

Dahlquist, J. A., Macchioli Grande, M., Alasino, P. H., Basei, M. A. S., Galindo, C., Moreno, J. A., & Morales Cámera, M. (2019). New geochronological and isotope data for the Las Chacras–Potrerillos and Renca batholiths: A contribution to the middle-upper Devonian magmatism in the pre-Andean foreland (Sierras Pampeanas, Argentina). SW Gondwana [Dataset]. Journal of South American Earth Sciences, *93*, 348–363. https://doi.org/10.1016/j.jsames.2019.04.026

Dahlquist, J. A., Morales Cámera, M. M., Alasino, P. H., Tickyj, H., Basei, M. A. S., Galindo, C., et al. (2020). Geochronology and geochemistry of Devonian magmatism in the Frontal Cordillera (Argentina): Geodynamic implications for the pre Andean SW Gondwana margin [Dataset]. International Geology Review, *64*(2), 2–21. https://doi.org/10.1080/00206814.2020.1845994

Dahlquist, J. A., Pankhurst, R. J., Gaschnig, R. M., Rapela, C. W., Casquet, C., Alasino, P. H., et al. (2013). Hf and Nd isotopes in Early Ordovician to Early Carboniferous granites as monitors of crustal growth in the Proto-Andean margin of Gondwana [Dataset]. Gondwana Research, *23*(4), 1617–1630. https://doi.org/10.1016/j.gr.2012.08.013

Dalla Salda, L., Cingolani, C., & Varela, R. (1991). El basamento pre-andino ígneo metamórfico de San Martín de los Andes, Neuquén [Dataset]. Revista de la Asociación Geológica Argentina, *46*(3–4), 223–234. http://naturalis.fcnym.unlp.edu.ar/id/000895

de Barrio, R. E., Recio, C., Ríos, F. J., Rolando, A. P., Del Blanco, M. A., & Schalamuk, I. B. (2023). Geology, geochemistry, isotope geochemistry and fluid inclusions of the Early Carboniferous granitic rocks from Bajo de La Leona, Deseado Massif (Santa Cruz, Argentina) and geological relationships with the Triassic-Jurassic magmatism. *Journal of South American Earth Sciences*, *123*, 104197. https://doi.org/10.1016/j.jsames.2023.104197

Dicaro, S., González, S. N., Serra-Varela, S., & Heredia, N. (2023). Structure and metamorphism of the cushamen complex in Sañicó and Collón Curá-limay rivers confluence: A Devonian metamorphic event related to the subduction stage of the gondwanan patagonian orogen. *Journal of South American Earth Sciences*, *121*, 104152. https://doi.org/10.1016/j.jsames.2022.104152

Dorais, M., Lira, R., Chen, Y., & Tingey, D. (1997). Origin of biotite–apatite-rich enclaves, Achala Batholith, Argentina [Dataset]. Contributions to Mineralogy and Petrology, *130*(1), 31–46. https://doi.org/10.1007/s004100050347

Du, L., Zhu, H., Yuan, C., Zhang, Y., Huang, Z., Li, X. P., & Long, X. (2021). Paleozoic crustal evolution and tectonic switching in the Northeastern Tianshan: Insights from zircon Hf isotopes of granitoids. *Journal of the Geological Society*, *178*(2), jgs2020. https://doi.org/10.1144/jgs2020-035

Duhart, P., Cardona, A., Valencia, V., Muñoz, J., Quiroz, D., & Hervé, F. (2009). Evidencias de basamento Devónico, Chile centro-sur 41–44°S. In *XII Congreso Geológico Chileno Servicio Nacional de Geología y Minería, Santiago, CD-ROM, S8_009*

Duhart, P., McDonough, M., Muñoz, J., Martin, M., & Villeneuve, M. (2001). El Complejo Metamórfico Bahía Mansa en la cordillera de la Costa del centro-sur de Chile (39° 30′–42° 00′S): geocronología K-Ar, 40Ar/39Ar y U/Pb e implicancias en la evolución del margen sur-Occidental de Gondwana [Dataset]. Revista Geologica de Chile, *28*(2), 179–208. https://doi.org/10.4067/S0716-02082001000200003

Escosteguy, L. D., Geuna, S. E., Franchi, M. L., González Diaz, E. F., & Dal Molin, C. N. (2013). Hoja Geológica 4172-II, San Martín de los Andes, Provincias de Río Negro y Neuquén. Retrieved from http://repositorio.segemar.gob.ar/handle/308849217/180

Falco, J. I., Hauser, N., Scivetti, N., Reimold, W. U., & Folguera, A. (2022). The origin of Patagonia: Insights from Permian to Middle Triassic magmatism of the North Patagonian Massif. *Geological Magazine*, *159*(9), 1490–1512. https://doi.org/10.1017/S0016756822000450

Folguera, A., & Ramos, V. A. (2011). Repeated eastward shifts of arc magmatism in the Southern Andes: A revision to the long-term pattern of Andean uplift and magmatism. *Journal of South American Earth Sciences*, *32*(4), 531–546. https://doi.org/10.1016/j.jsames.2011.04.003

Forsythe, R. (1982). The late Palaeozoic to early Mesozoic evolution of southern South America: A plate tectonic interpretation. *Journal of the Geological Society*, *139*(6), 671–682. https://doi.org/10.1144/gsjgs.139.6.0671

Franzese, J. R. (1995). El Complejo Piedra Santa (Neuquén, Argentina): parte de un cinturón metamórfico neopaleozoico del Gondwana surooccidental [Dataset]. Andean Geology, *22*(2), 193e202.http://andeangeology.cl/index.php/revista1/article/view/V22n2-a04

Galli, C. A. (1969). *Descripción geológica de la hoja 38e, Piedra del Águila. Provincias de Neuquén y de Río Negro* (Vol. 111). Dirección Nacional de Geololgía y Minería, Boletín. Retrieved from http://repositorio.segemar.gov.ar/308849217/534

Garber, J. M., Roeske, S. M., Warren, J., Mulcahy, S. R., McClelland, W. C., Austin, L. J., et al. (2014). Crustal shortening, exhumation, and strain localization in a collisional orogen: The Bajo Pequeño Shear Zone, Sierra de Pie de Palo, Argentina [Dataset]. Tectonics, *33*(7), 1277–1303. https://doi.org/10.1002/2013TC003477

García-Sansegundo, J., Farias, P., Gallastegui, G., Giacosa, R. E., & Heredia, N. (2009). Structure and metamorphism of the Gondwanan basement in the Bariloche region (North Patagonian Argentine Andes). *International Journal of Earth Sciences*, *98*(7), 1599–1608. https://doi.org/10.1007/s00531-008-0330-3

Gianni, G. M., Dávila, F. M., Echaurren, A., Fennell, L., Tobal, J., Navarrete, C., et al. (2018). A geodynamic model linking Cretaceous orogeny, arc migration, foreland dynamic subsidence and marine ingression in southern South America. *Earth-Science Reviews*, *185*, 437–462. https://doi.org/10.1016/j.earscirev.2018.06.016

Gianni, G. M., & Pérez Luján, S. (2021). Geodynamic controls on magmatic arc migration and quiescence. *Earth-Science Reviews*, *218*, 103676. https://doi.org/10.1016/j.earscirev.2021.103676

González, P. D., & Giacosa, R. (2022). Rocas metamórficas e ígneas del Paleozoico. In *XXI Congreso geológico Argentino. Capítulo B.1* (pp. 47–104).

González, P. D., Naipauer, M., Sato, A. M., Varela, R., Basei, M. A., Cábana, M. C., et al. (2021). Early Paleozoic structural and metamorphic evolution of the Transpatagonian Orogen related to Gondwana assembly. *International Journal of Earth Sciences*, *110*(1), 81–111. https://doi.org/10.1007/s00531-020-01939-0

González, P. D., Sato, A. M., Naipauer, M., Varela, R., Basei, M., Sato, K., et al. (2018). Patagonia-Antarctica Early Paleozoic conjugate margins: Cambrian synsedimentary silicic magmatism, U/Pb dating of K-bentonites, and related volcanogenic rocks. *Gondwana Research*, *63*, 186–225. https://doi.org/10.1016/j.gr.2018.05.015

Greco, G. A., González, P. D., González, S. N., Sato, A. M., Basei, M. A. S., Tassinari, C. C. G., et al. (2015). Geology, structure, and age of the Nahuel Niyeu formation in the Aguada Cecilio area, North Patagonian Massif, Argentina. *Journal of South American Earth Sciences*, *62*, 12–32. https://doi.org/10.1016/j.jsames.2015.04.005

Greco, G. A., González, S. N., Sato, A. M., González, P. D., Basei, M. A., Llambías, E. J., & Varela, R. (2017). The Nahuel Niyeu basin: A Cambrian forearc basin in the eastern North Patagonian Massif. *Journal of South American Earth Sciences*, *79*, 111–136. https://doi.org/10.1016/j.jsames.2017.07.009

Gregori, D. A., Kostadinoff, J., Strazzere, L., & Raniolo, A. (2008). Tectonic significance and consequences of the Gondwanide orogeny in northern Patagonia, Argentina. *Gondwana Research*, *14*(3), 429–450. https://doi.org/10.1016/j.gr.2008.04.005

Gregori, D. A., Strazzere, L., Barros, M., Benedini, L., Marcos, P., & Kostadinoff, J. (2020). The Mencué batholith: Permian episodic arc-related magmatism in the western North Patagonian Massif, Argentina. *International Geology Review*, *63*(3), 1–25. https://doi.org/10.1080/00206814.2019.1710865

Griffin, W. L., Wang, X., Jackson, S. E., Pearson, N. J., O'Reilly, S. Y., Xu, X., & Zhou, X. (2002). Zircon chemistry and magma mixing, SE China: In-situ analysis of Hf isotopes, Tonglu and Pingtan igneous complexes [Dataset]. Lithos, *61*(3–4), 237–269. https://doi.org/10.1016/S0024-4937(02)00082-8

Hawkesworth, C., Cawood, P. A., & Dhuime, B. (2019). Rates of generation and growth of the continental crust. *Geoscience Frontiers*, *10*(1), 165–173. https://doi.org/10.1016/j.gsf.2018.02.004

Hawkesworth, C. J., Dhuime, B., Pietranik, A. B., Cawood, P. A., Kemp, A. I., & Storey, C. D. (2010). The generation and evolution of the continental crust. *Journal of the Geological Society*, *167*(2), 229–248. https://doi.org/10.1144/0016-76492009-072

Heredia, N., García-Sansegundo, J., Gallastegui, G., Farias, P., Giacosa, R. E., Alonso, J. L., et al. (2016). *Evolución geodinámica de los Andes de Argentina, Chile y la Península Antártica durante el Neoproterozoico superior y el Paleozoico* (Vol. 36, pp. 237–278). Trabajos de Geología, Universidad de Oviedo. https://doi.org/10.17811/tdg.36.2016.237-278

Hervé, F., Calderon, M., Fanning, C. M., Pankhurst, R. J., Fuentes, F., Rapela, C. W., et al. (2016). Devonian magmatism in the accretionary complex of southern Chile [Dataset]. Journal of the Geological Society, *173*, 587–602. https://doi.org/10.1144/jgs2015-163

Hervé, F., Calderón, M., Fanning, C. M., Pankhurst, R. J., & Godoy, E. (2013). Provenance variations in the Late Paleozoic accretionary complex of central Chile as indicated by detrital zircons [Dataset]. Gondwana Research, *23*(3), 1122–1135. https://doi.org/10.1016/j.gr.2012.06.016

Hervé, F., Calderón, M., Fanning, M., Pankhurst, R., Rapela, C. W., & Quezada, P. (2018). The country rocks of Devonian magmatism in the North Patagonian Massif and Chaitenia [Dataset]. Andean Geology, *45*(3), 301–317. https://doi.org/10.5027/andgeoV45n3-3117

Hervé, F., Pankhurst, R. J., Brook, M., Alfaro, G., Frutos, J., Miller, H., et al. (1990). Rb-Sr and Sm-Nd data from some massive sulfide occurrences in the metamorphic basement of South-Central Chile [Dataset]. Stratabound ore deposits in the Andes (pp. 221–228). Springer. Retrieved from https://link.springer.com/chapter/10.1007/978-3-642-88282-1_16

Hoskin, P. W. O., & Black, L. P. (2000). Metamorphic zircon formation by solid-state recrystallization of protolith igneous zircon. *Journal of Metamorphic Geology*, *18*(4), 423–439. https://doi.org/10.1046/j.1525-1314.2000.00266.x

Hyppolito, T., García-Casco, A., Juliani, C., Meira, V. T., & Hall, C. (2014). Late Paleozoic onset of subduction and exhumation at the western margin of Gondwana (Chilenia Terrane): Counterclockwise P–T paths and timing of metamorphism of deep-seated garnet–mica schist and amphibolite of Punta Sirena, Coastal Accretionary Complex, central Chile (34°S). *Lithos*, *206*, 409–434. https://doi.org/10.1016/j.lithos.2014.07.023

Iizuka, T., Hirata, T., Komiya, T., Rino, S., Katayama, I., Motoki, A., & Maruyama, S. (2005). U-Pb and Lu-Hf isotope systematics of zircons from the Mississippi River sand: Implications for reworking and growth of continental crust. *Geology*, *33*(6), 485–488. https://doi.org/10.1130/G21427.1

Iizuka, T., Yamaguchi, T., Itano, K., Hibiya, Y., & Suzuki, K. (2017). What Hf isotopes in zircon tell us about crust–mantle evolution. *Lithos*, *274*, 304–327. https://doi.org/10.1016/j.lithos.2017.01.006

Kato, T. T., Sharp, W. D., & Godoy, E. (2008). Inception of a Devonian subduction zone along the southwestern Gondwana margin: 40Ar–39Ar dating of eclogite–amphibolite assemblages in blueschist boulders from the Coastal range of Chile (41°S) [Dataset]. Canadian Journal of Earth Sciences, *45*(3), 337–351. https://doi.org/10.1139/E08-006

Kato, T. T., Sharp, W. D., & Godoy, E. (2009). Devonian-Carboniferous retro-eclogite (blueschist) boulders from the Cordillera de la Costa accretionary complex (41 o S), Chile: Tectonic similarities to high grade blueschists of the California Coast Ranges, USA [Dataset]. XII Congreso Geológico Chileno (Santiago, 22–26 Noviembre, 2009), S8_018. (p. 4). Retrieved from https://catalogobiblioteca.sernageomin.cl/Archivos/12993_v2_S8_018.pdf

Kemp, A. I. S., Hawkesworth, C. J., Collins, W. J., Gray, C. M., & Blevin, P. L. (2009). Isotopic evidence for rapid continental growth in an extensional accretionary orogen: The Tasmanides, eastern Australia. *Earth and Planetary Science Letters*, *284*(3–4), 455–466. https://doi.org/10.1016/j.epsl.2009.05.011

Kemp, A. I. S., Hawkesworth, C. J., Foster, G. L., Paterson, B. A., Woodhead, J. D., Hergt, J. M., et al. (2007). Magmatic and crustal differentiation history of granitic rocks from Hf-O isotopes in zircon. *Science*, *315*(5814), 980–983. https://doi.org/10.1126/science.1136154

Kemp, A. I. S., Hawkesworth, C. J., Paterson, B. A., & Kinny, P. D. (2006). Episodic growth of the Gondwana supercontinent from hafnium and oxygen isotopes in zircon. *Nature*, *439*(7076), 580–583. https://doi.org/10.1038/nature04505

Kinny, P. D., & Maas, R. (2003). Lu–Hf and Sm–Nd isotope systems in zircon. *Reviews in Mineralogy and Geochemistry*, *53*(1), 327–341. https://doi.org/10.2113/0530327

Kröner, A., Kovach, V., Belousova, E., Hegner, E., Armstrong, R., Dolgopolova, A., et al. (2014). Reassessment of continental growth during the accretionary history of the Central Asian Orogenic belt. *Gondwana Research*, *25*(1), 103–125. https://doi.org/10.1016/j.gr.2012.12.023

Li, X. H., Li, Z. X., He, B., Li, W. X., Li, Q. L., Gao, Y., & Wang, X. C. (2011). The Early Permian active continental margin and crustal growth of the Cathaysia Block: In situ U–Pb, Lu–Hf and O isotope analyses of detrital zircons. *Chemical Geology*, *328*, 195–207. https://doi.org/10.1016/j.chemgeo.2011.10.027

Linares, E., Cagnoni, M. C., Do Campo, M., & Ostera, H. A. (1988). Geochronology of metamorphic and eruptive rocks of southeastern Neuquén and northwestern Río Negro Provinces, Argentine Republic [Dataset]. Journal of South American Earth Sciences, *1*(1), 53–61. https://doi.org/10.1016/0895-9811(88)90015-6

Löbens, S., Oriolo, S., Benowitz, J., Wemmer, K., Layer, P., & Siegesmund, S. (2017). Late Paleozoic deformation and exhumation in the Sierras Pampeanas (Argentina): 40Ar/39Ar-feldspar dating constraints. *International Journal of Earth Sciences*, *106*(6), 1991–2003. https://doi.org/10.1007/s00531-016-1403-3

López, V. L., & Gregori, D. A. (2004). Provenance and evolution of the Guarguaráz Complex, Cordillera Frontal, Argentina. *Gondwana Research*, *7*(4), 1197–1208. https://doi.org/10.1016/S1342-937X(05)71093-5

López de Luchi, M. G., Cerredo, M. E., & Martínez Dopico, C. (2010). Lithology and age of the Cushamen formation. Devonian magmatism in the western North Patagonian Massif. Argentina. Bolletino di Geofisica Teorica. *Applicata*, *51*, 71–74.

López de Luchi, M. G. L., Siegesmund, S., Wemmer, K., & Nolte, N. (2017). Petrogenesis of the postcollisional Middle Devonian monzonitic to granitic magmatism of the Sierra de San Luis, Argentina [Dataset]. Lithos, *288*, 191–213. https://doi.org/10.1016/j.lithos.2017.05.018

Lucassen, F., Trumbull, R., Franz, G., Creixell, C., Vásquez, P., Romer, R. L., & Figueroa, O. (2004). Distinguishing crustal recycling and juvenile additions at active continental margins: The Paleozoic to recent compositional evolution of the Chilean Pacific margin (36–41 S) [Dataset]. Journal of South American Earth Sciences, *17*(2), 103–119. https://doi.org/10.1016/j.jsames.2004.04.002

Marcos, P. (2020). *Los basamentos famatinianos y gondwanicos del sector occidental del norte de Patagonia* (pp. 11–188). Tesis Doctoral, Universidad Nacional del Sur, Departamento de Geología. Bahía Blanca, Argentina Retrieved from http://repositoriodigital.uns.edu.ar/handle/123456789/5356

Marcos, P., Gregori, D. A., Benedini, L., Barros, M., Strazzere, L., & Pivetta, C. P. (2018). Pennsylvanian glacimarine sedimentation in the Cushamen formation, western North Patagonian Massif. *Geoscience Frontiers*, *9*(2), 485–504. https://doi.org/10.1016/j.gsf.2017.05.005

Marcos, P., Pivetta, C. P., Benedini, L., Gregori, D. A., Geraldes, M., Scivetti, N., et al. (2020). Late Paleozoic geodynamic evolution of the western North Patagonian Massif and its tectonic context along the southwestern Gondwana margin. *Lithos*, *376*, 105801. https://doi.org/10.1016/j.lithos.2020.105801

Martin, M. W., Kato, T. T., Rodriguez, C., Godoy, E., Duhart, P., McDonough, M., & Campos, A. (1999). Evolution of the late Paleozoic accretionary complex and overlying forearc-magmatic arc, south central Chile (38°–41°S): Constraints for the tectonic setting along the southwestern margin of Gondwana. *Tectonics*, *18*(4), 582–605. https://doi.org/10.1029/1999TC900021

Martínez, J. C., Dristas, J. A., & Massonne, H. J. (2012). Palaeozoic accretion of the microcontinent Chilenia, North Patagonian Andes: High-pressure metamorphism and subsequent thermal relaxation [Dataset]. International Geology Review, *54*(4), 472–490. https://doi.org/10.1080/00206814.2011.569411

Massonne, H. J., & Calderón, M. (2008). PT evolution of metapelites from the Guarguaraz Complex, Argentina: Evidence for Devonian crustal thickening close to the western Gondwana margin. *Revista Geológica de Chile*, *35*(2), 215–231. https://doi.org/10.4067/s0716-02082008000200002

Morales Cámera, M. M., Dahlquist, J. A., García-Arias, M., Moreno, J. A., Galindo, C., Basei, M. A. S., & Molina, J. F. (2020). Petrogenesis of the F-rich peraluminous A-type granites: An example from the devonian achala batholith (Characato Suite), Sierras Pampeanas, Argentina [Dataset]. Lithos, *378–379*, 105792. https://doi.org/10.1016/j.lithos.2020.105792

Morales Cámera, M. M., Dahlquist, J. A., Ramacciotti, C. D., Galindo, C., Basei, M. A. S., Zandomeni, P. S., & Macchioli Grande, M. (2018). The strongly peraluminous A-type granites of the Characato suite (Achala batholith), Sierras Pampeanas, Argentina: Evidence of Devonian-Carboniferous crustal reworking [Dataset]. Journal of South American Earth Sciences, *88*, 551–567. https://doi.org/10.1016/j.jsames.2018.09.008

Morosini, A. F., Suárez, A. E. O., Otamendi, J. E., Pagano, D. S., & Ramos, G. A. (2017). La Escalerilla pluton, San Luis Argentina: The orogenic and post-orogenic magmatic evolution of the famatinian cycle at Sierras de San Luis [Dataset]. Journal of South American Earth Sciences, *73*, 100–118. https://doi.org/10.1016/j.jsames.2016.12.001

Mosquera, A., & Ramos, V. A. (2006). Intraplate deformation in the Neuquén Embayment. *Special Papers - Geological Society of America*, *407*, 97. https://doi.org/10.1130/2006.2407(05

Nebel, O., Vroon, P. Z., van Westrenen, W., Iizuka, T., & Davies, G. R. (2011). The effect of sediment recycling in subduction zones on the Hf isotope character of new arc crust, Banda arc, Indonesia. *Earth and Planetary Science Letters*, *303*(3–4), 240–250. https://doi.org/10.1016/j.epsl.2010.12.053

Nelson, D. A., & Cottle, J. M. (2018). The secular development of accretionary orogens: Linking the Gondwana magmatic arc record of West Antarctica, Australia and South America. *Gondwana Research*, *63*, 15–33. https://doi.org/10.1016/j.gr.2018.06.002

Oriolo, S., González, P. D., Renda, E. M., Basei, M. A., Otamendi, J., Cordenons, P., et al. (2023). Linking accretionary orogens with continental crustal growth and stabilization: Lessons from Patagonia [Dataset]. Gondwana Research, *121*, 368–382. https://doi.org/10.1016/j.gr.2023.05.011

Oriolo, S., Schulz, B., Geuna, S., González, P. D., Otamendi, J. E., Sláma, J., et al. (2021). Early Paleozoic accretionary orogens along the western Gondwana margin. *Geoscience Frontiers*, *12*(1), 109–130. https://doi.org/10.1016/j.gsf.2020.07.001

Oriolo, S., Schulz, B., González, P. D., Bechis, F., Olaizola, E., Krause, J., et al. (2019). The Late Paleozoic tectonometamorphic evolution of Patagonia revisited: Insights from the pressure-temperature-deformation-time (P-T-D-t) path of the Gondwanide basement of the North Patagonian Cordillera (Argentina). *Tectonics*, *38*(7), 2378–2400. https://doi.org/10.1029/2018TC005358

Ostera, H. A., Linares, E., Haller, M. J., Cagnoni, M. C., & López de Luchi, M. (2001). A widespread Devonian Metamorphic episode in Northern Patagonia, Argentina. II South American Symposium on isotope Geology (Sociedad Geológica de Chile, Santiago). *Extended Abstracts Volume (CD)*, 600–603.

Palape, C., Quezada, P., Bastías, J., Hervé, F., Reyes, T., Veas, M., et al. (2022). Forearc tectonics and volcanism during the Devonian–Carboniferous evolution of the North Patagonian segment, southern Chile (41, 3°S). *Frontiers in Earth Science*, *10*, 873785. https://doi.org/10.3389/feart.2022.873785

Pankhurst, R. J., Rapela, C. W., Fanning, C. M., & Márquez, M. (2006). Gondwanide continental collision and the origin of Patagonia [Dataset]. Earth-Science Reviews, *76*, 235–257. https://doi.org/10.1016/j.earscirev.2006.02.001

Pankhurst, R. J., Rapela, C. W., Loske, W. P., Márquez, M., & Fanning, C. M. (2003). Chronological study of the pre-Permian basement rocks of southern Patagonia. *Journal of South American Earth Sciences*, *16*(1), 27–44. https://doi.org/10.1016/S0895-9811(03)00017-8

Pietranik, A. B., Hawkesworth, C. J., Storey, C. D., Kemp, A. I. S., Sircombe, K. N., Whitehouse, M. J., & Bleeker, W. (2008). Episodic, mafic crust formation from 4.5 to 2.8 Ga: New evidence from detrital zircons, Slave craton, Canada [Dataset]. Geology, *36*(11), 875–878. https://doi.org/10.1130/G24861A.1

Plissart, G., González-Jiménez, J. M., Garrido, L. N., Colás, V., Berger, J., Monnier, C., et al. (2019). Tectono-metamorphic evolution of subduction channel serpentinites from South-Central Chile. *Lithos*, *336*, 221–241. https://doi.org/10.1016/j.lithos.2019.03.023

Quezada Pozo, P. A. (2015). *Geología del basamento de la Región de los Lagos, Chile; evidencias de magmatismo calco-alcalino y aportes sedimentarios devónicos. Memoria para optar al título de Geólogo*. Universidad de Chile, Departamento de Geología, Facultad de Ciencias Físicas y Matemáticas. IX + 86 p., Santiago de Chile Retrieved from http://repositorio.uchile.cl/handle/2250/133541

Ramos, V. A. (1984). Patagonia: un continente paleozoico a la deriva? In *9 Congreso Geologico Argentino* (pp. 311–325). SC Bariloche.

Ramos, V. A. (2008). Patagonia: A Paleozoic continent adrift? *Journal of South American Earth Sciences*, *26*(3), 235–251. https://doi.org/10.1016/j.jsames.2008.06.002

Ramos, V. A., Dallmeyer, R. D., & Vujovich, G. (1998). Time constraints on the early Palaeozoic docking of the Precordillera, central Argentina [Dataset]. Geological Society, London, Special Publications, *142*, 143–158. https://doi.org/10.1144/GSL.SP.1998.142.01.08

Ramos, V. A., Jordan, T. E., Allmendinger, R. W., Mpodozis, C., Kay, S. M., Cortés, J. M., & Palma, M. (1986). Paleozoic terranes of the central Argentine-Chilean Andes. *Tectonics*, *5*(6), 855–880. https://doi.org/10.1029/TC005i006p00855

Ramos, V. A., Lovecchio, J. P., Naipauer, M., & Pángaro, F. (2020). The collision of Patagonia: Geological facts and speculative interpretations. *Ameghiniana*, *57*(5), 464–479. https://doi.org/10.5710/AMGH.27.05.2020.3352

Ramos, V. A., & Naipauer, M. (2014). Patagonia: Where does it come from? *Journal of Iberian Geology*, *40*(2), 367–379. https://doi.org/10.5209/rev_JIGE.2014.v40.n2.45304

Rapalini, A. E., Lopez de Luchi, M., Martinez Dopico, C., Lince Klinger, F., Gimenez, M. E., & Martinez, M. P. (2010). Did Patagonia collide against Gondwana in the Late Paleozoic? Some insights from a multidisciplinary study of magmatic units of the North Patagonian Massif. *Geológica Acta*, *8*, 349–371.

Rapalini, A. E., Luchi, M. L., Tohver, E., & Cawood, P. A. (2013). The South American ancestry of the North Patagonian Massif: Geochronological evidence for an autochthonous origin? *Terra Nova*, *25*(4), 337–342. https://doi.org/10.1111/ter.12043

Rapela, C. W., Baldo, E. G., Pankhurst, R. J., & Fanning, C. M. (2008). The Devonian Achala batholith of the Sierras Pampeanas: F-rich, aluminous A-type granites. In *VI South American symposium on isotope Geology (San Carlos de Bariloche, 13–17 Abril, 2008)* (Vol. 1, pp. 104–111).

Rapela, C. W., Hervé, F., Pankhurst, R. J., Calderón, M., Fanning, C. M., & Quezada, P. (2022). The Chaitenia accretionary orogeny of northwest Patagonia: New U-Pb SHRIMP ages of the foreland. In *XXI Congreso Geológico Argentino*. (pp. 1511–1512).

Rapela, C. W., Hervé, F., Pankhurst, R. J., Calderón, M., Fanning, C. M., Quezada, P., et al. (2021). The Devonian accretionary orogen of the North Patagonian cordillera [Dataset]. Gondwana Research, *96*, 1–21. https://doi.org/10.1016/j.gr.2021.04.004

Renda, E. M., Alvarez, D., Prezzi, C., Oriolo, S., & Vizán, H. (2019). Inherited basement structures and their influence in foreland evolution: A case study in Central Patagonia, Argentina. *Tectonophysics*, *772*, 228232. https://doi.org/10.1016/j.tecto.2019.228232

Renda, E. M., Baumgartner, L., Putlitz, B., González, P. D., Oriolo, S., & Marcos, P. (2022). High grade metamorphism in central Patagonia (Argentina) associated with an accretionary orogeny. [Dataset]. Metamorphic Studies Group meeting. Mineralogical Society. Retrieved from https://rid.unrn.edu.ar/handle/20.500.12049/8287

Renda, E. M., González, P. D., Vizán, H., Oriolo, S., Prezzi, C., Ruiz González, V., et al. (2021). Igneous-metamorphic basement of Taquetrén range, Patagonia, Argentina: A key locality for the reconstruction of the Paleozoic evolution of Patagonia [Dataset]. Journal of South American Earth Sciences, *106*, 103045. https://doi.org/10.1016/j.jsames.2020.103045

Richter, P. P., Ring, U., Willner, A. P., & Leiss, B. (2007). Structural contacts in subduction complexes and their tectonic significance: The Late Palaeozoic coastal accretionary wedge of central Chile. *Journal of the Geological Society*, *164*(1), 203–214. https://doi.org/10.1144/0016-76492005-181

Roberts, N. M., & Spencer, C. J. (2015). The zircon archive of continent formation through time. *Geological Society, London, Special Publications*, *389*(1), 197–225. https://doi.org/10.1144/SP389.14

Rojo, D., Calderón, M., Hervé, F., Díaz, J., Quezada, P., Suárez, R., et al. (2021). Petrology and tectonic evolution of late Paleozoic mafic-ultramafic sequences and the Leones Pluton of the eastern Andean Metamorphic Complex (46-47° S), southern Chile. *Journal of South American Earth Sciences*, *108*, 103198. https://doi.org/10.1016/j.jsames.2021.103198

Rubatto, D. (2002). Zircon trace element geochemistry: Partitioning with garnet and the link between U–Pb ages and metamorphism. *Chemical Geology*, *184*(1–2), 123–138. https://doi.org/10.1016/S0009-2541(01)00355-2

Sawyer, E. W., & Brown, M. (2008). In *Working with migmatites. Mineralogical association of Canada* (Vol. 38, p. 168).

Scherer, E. E., Whitehouse, M. J., & Munker, C. (2007). Zircon as a monitor of crustal growth. *Elements*, *3*(1), 19–24. https://doi.org/10.2113/gselements.3.1.19

Serra-Varela, S., González, P. D., Giacosa, R., Heredia, N., Pedreira, D., Martín-González, F., & Sato, A. (2019). Evolution of the Palaeozoic basement of the Northpatagonian Andes in the San Martín de los Andes area (Neuquén, Argentina): Petrology, age and correlations [Dataset]. Andean Geology, *46*, 102. https://doi.org/10.5027/andgeoV46n1-3124

Serra-Varela, S., Heredia, N., Giacosa, R., García-Sansegundo, J., & Farias, P. (2020). Review of the polyorogenic Paleozoic basement of the Argentinean North Patagonian Andes: Age, correlations, tectonostratigraphic interpretation and geodynamic evolution. *International Geology Review*, *64*(1), 72–95. https://doi.org/10.1080/00206814.2020.1839798

Serra-Varela, S., Heredia, N., Otamendi, J., & Giacosa, R. (2021). Petrology and geochronology of the San Martín de los Andes batholith: Insights into the Devonian magmatism of the North Patagonian Andes [Dataset]. Journal of South American Earth Sciences, *109*, 103283. https://doi.org/10.1016/j.jsames.2021.103283

Siegesmund, S., Steenken, A., López de Luchi, M. G., Wemmer, K., Hoffmann, A., & Mosch, S. (2004). The Las Chacras-Potrerillos batholith (Pampean ranges, Argentina): Structural evidences, emplacement and timing of the intrusion [Dataset]. International Journal of Earth Sciences, *93*, 23–43. https://doi.org/10.1007/s00531-003-0363-6

Steenken, A., Wemmer, K., Martino, R. D., López de Luchi, M. G., Guereschi, A., & Siegesmund, S. (2010). Post-Pampean cooling and the uplift of the Sierras Pampeanas in the west of Córdoba (Central Argentina) [Dataset]. N Jb Geol Paläont Abh, *256*(2), 235–255. https://doi.org/10.1127/0077-7749/2010/0094

Stuart-Smith, P. G., Camacho, A., Sims, J. P., Skirrow, R. G., Lyons, P., Pieters, P. E., et al. (1999). Uranium-lead dating of felsic magmatic cycles in the southern Sierras Pampeanas, Argentina; implications for the tectonic development of the proto-Andean Gondwana margin. [Dataset]. In V. A. Ramos, & J. D. Keppie (Eds.), Laurentia- Gondwana connections before Pangea Special Papers of the Geological Society of America. (Vol. *336*, pp. 87–114). https://doi.org/10.1130/0-8137-2336-1.87

Suárez, R., Ghiglione, M. C., Sue, C., Quezada, P., Roy, S., Rojo, D., & Calderón, M. (2021). Paleozoic-early Mesozoic structural evolution of the West Gondwana accretionary margin in southern Patagonia, Argentina. *Journal of South American Earth Sciences*, *106*, 103062. https://doi.org/10.1016/j.jsames.2020.103062

Suárez, R., González, P. D., & Ghiglione, M. C. (2019). A review on the tectonic evolution of the Paleozoic-Triassic basins from Patagonia: Record of protracted westward migration of the pre-Jurassic subduction zone. *Journal of South American Earth Sciences*, *95*, 102256. https://doi.org/10.1016/j.jsames.2019.102256

Tickyj, H., Basei, M. A. S., & Tomezzoli, R. N. (2017). Edades U-Pb en circones de plutones del Cordón del Carrizalito, Cordillera Frontal. In *XX Congreso Geológico Argentino. Simposio 13: Tectónica pre-Andina*. (p. 161).

Tickyj, H., Tomezzoli, R. N., Basei, M. A., Fernández, M. A., Blatter, J. M., Rodríguez, N., & Gallo, L. C. (2015). Geología de la Formación Piedras de Afilar, basamento granítico del Distrito Minero Agua Escondida, Mendoza. In *III Simposio de Petrología Ignea y Metalogénesis Asociada, General Roca, Argentina. CD Resúmenes*. (pp. 158–159).

Urraza, I. A., Delpino, S. H., & Grecco, L. E. (2019). MORB-derived amphibolites in the Paleozoic basement of the Aluminé Igneous-Metamorphic Complex, Neuquén, Argentina: Decoding its genesis, PT evolution and pre-Andean regional correlations [Dataset]. Geológica Acta, *17*, 1–24. https://doi.org/10.1344/GeologicaActa2019.17.10

Varela, R., Basei, M. A., Cingolani, C. A., Siga, O., Jr., & Passarelli, C. R. (2005). El basamento cristalino de los Andes norpatagónicos en Argentina: Geocronología e interpretación tectónica. *Revista Geológica de Chile*, *32*(2), 167–187. https://doi.org/10.4067/s0716-02082005000200001

Varela, R., Dalla Salda, L. H., Cingolani, C. A., & Gomez, V. (1991). Estructura, petrología y geocronología del basamento de la región del Limay, provincias de Río Negro y Neuquen, Argentina. *Revista Geológica de Chile*, *18*, 147–163.

von Gosen, W. (2009). Stages of Late Palaeozoic deformation and intrusive activity in the western part of the North Patagonian Massif (southern Argentina) and their geotectonic implications. *Geological Magazine*, *146*(1), 48–71. https://doi.org/10.1017/S0016756808005311

Wang, C. Y., Campbell, I. H., Allen, C. M., Williams, I. S., & Eggins, S. M. (2009). Rate of growth of the preserved North American continental crust: Evidence from Hf and O isotopes in Mississippi detrital zircons. *Geochimica et Cosmochimica Acta*, *73*(3), 712–728. https://doi.org/10.1016/j.gca.2008.10.037

Whitney, D. L., & Evans, B. W. (2010). Abbreviations for names of rock-forming minerals. *American Mineralogist*, *95*(1), 185–187. https://doi.org/10.2138/am.2010.3371

Willner, A. P., Anczkiewicz, R., Glodny, J., Pohlner, J. E., Sudo, M., van Staal, C. R., & Vujovich, G. I. (2023). Interrelated pressure-temperature-time-paths of medium to high pressure metamorphic rocks in the Sierra Pie de Palo (W-Argentina): Evolution of a "hard" collisional wedge during an Ordovician microcontinent-arc collision. *Tectonophysics*, *859*, 229861. https://doi.org/10.1016/j.tecto.2023.229861

Willner, A. P., Gerdes, A., & Massonne, H. J. (2008). History of crustal growth and recycling at the Pacific convergent margin of South America at latitudes 29°–36° S revealed by a U–Pb and Lu–Hf isotope study of detrital zircon from late Paleozoic accretionary systems. *Chemical Geology*, *253*(3–4), 114–129. https://doi.org/10.1016/j.chemgeo.2008.04.016

Willner, A. P., Gerdes, A., Massonne, H. J., Schmidt, A., Sudo, M., Thomson, S. N., & Vujovich, G. (2011). The geodynamics of collision of a microplate (Chilenia) in Devonian times deduced by the pressure–temperature–time evolution within part of a collisional belt (Guarguaraz Complex, W-Argentina) [Dataset]. Contributions to Mineralogy and Petrology, *162*, 303–327. https://doi.org/10.1007/s00410-010-0598-8

Willner, A. P., Glodny, J., Gerya, T. V., Godoy, E., & Massonne, H. J. (2004). A counterclockwise PTt path of high-pressure/low-temperature rocks from the Coastal Cordillera accretionary complex of south-central Chile: Constraints for the earliest stage of subduction mass flow [Dataset]. Lithos, *75*(3–4), 283–310. https://doi.org/10.1016/j.lithos.2004.03.002

Willner, A. P., Thomson, S. N., Kröner, A., Wartho, J. A., Wijbrans, J. R., & Hervé, F. (2005). Time markers for the evolution and exhumation history of a Late Palaeozoic paired metamorphic belt in North–Central Chile (34–35 30′S) [Dataset]. Journal of Petrology, *46*, 1835–1858. https://doi.org/10.1093/petrology/egi036

Wu, G., Yang, S., Liu, W., Nance, R. D., Chen, X., Wang, Z., & Xiao, Y. (2021). Switching from advancing to retreating subduction in the Neoproterozoic Tarim Craton, NW China: Implications for Rodinia breakup. *Geoscience Frontiers*, *12*(1), 161–171. https://doi.org/10.1016/j.gsf.2020.03.013

Yoya, M. B., Oriolo, S., González, P., Restelli, F., Renda, E., Bechis, F., et al. (2023). The birth of the Gondwanide arc: Insights into Carboniferous magmatism of the North Patagonian Andes (Argentina). *Journal of South American Earth Sciences*, *123*, 104225. https://doi.org/10.1016/j.jsames.2023.104225

Zhang, X., Chung, S. L., Lai, Y. M., Ghani, A. A., Murtadha, S., Lee, H. Y., & Hsu, C. C. (2019). A 6000-km-long Neo-Tethyan arc system with coherent magmatic flare-ups and lulls in South Asia. *Geology*, *47*(6), 573–576. https://doi.org/10.1130/G46172.1

References From the Supporting Information

Alves, M. I., Almeida, B. S., Cardoso, L. M. C., Santos, A. C., Appi, C., Bertotti, A. L., et al. (2019). Isotopic composition of Lu, Hf and Yb in GJ-1, 91500 and Mud Tank reference materials measured by LA-ICP-MS: Application of the Lu-Hf geochronology in zircon [Dataset]. Journal of Sedimentary Environments, *4*(2), 220–248. https://doi.org/10.12957/jse.2019.43877

Basei, M., Ramos, V. A., Vujovich, G. I., & Poma, S. (1998). El basamento metamórfico de la Cordillera Frontal de Mendoza: nuevos datos geocronológicos e isotópicos. In *Congreso Latinoamericano de Geología*. (Vol. 10, pp. 412–417).

Bertotti, A. L., Chemale, F., & Kawashita, K. (2013). Lu-Hf em Zircão por LA-ICP-MS: Aplicação em Gabro do Ofiolito de Aburrá, Colômbia [Dataset]. Pesquisas em Geociencias, *40*, 117–127. https://doi.org/10.22456/1807-9806.43075

Bouvier, A., Vervoort, J. D., & Patchett, P. J. (2008). The Lu–Hf and Sm–Nd isotopic composition of CHUR: Constraints from unequilibrated chondrites and implications for the bulk composition of terrestrial planets [Dataset]. Earth and Planetary Science Letters, *273*, 48–57. https://doi.org/10.1016/j.epsl.2008.06.010

Choi, S. H., Mukasa, S. B., Andronikov, A., Osanai, Y., Harley, S., & Kelly, N. (2006). Lu–Hf systematics of the ultra-high temperature Napier Metamorphic Complex in Antarctica: Evidence for the early Archean differentiation of Earth's mantle [Dataset]. Earth and Planetary Science Letters, *246*(3–4), 305–316. https://doi.org/10.1016/j.epsl.2006.04.012

Davis, J. S., Moores, E. M., Roeske, S. M., Kay, S. M., McLelland, W. C. R., & Snee, L. W. (1995). New data from the western margin of Precordillera terrane, Argentina: Constrain scenarios for the middle Paleozoic tectonics of western South America. In *Laurentian- Gondwanan connections before Pangea field Conference, Program with Abstracts*. (Vol. 15–16).

DePaolo, D. J., Linn, A. M., & Schubert, G. (1991). The continental crustal age distribution. Methods of determining mantle separation ages from Sm-Nd isotopic data and application to the Southwestern United States [Dataset]. Journal of Geophysical Research, *96*(B2), 2071–2088. https://doi.org/10.1029/90JB02219

Dessanti, R. N., & Caminos, R. L. (1967). Edades Potasio-Argón y Posición Geológica de Algunas Rocas Igneas y Metamórficas de la Precordillera, Cordillera Frontal y Sierras de San Rafael, Provincia de Mendoza. *Revista de la Asociación Geológica Argentina*, *22*, 135–162.

Duchene, S., Blichert-Toft, J., Luais, B., Telouk, P., & Albarede, F. (1997). The Lu–Hf dating of garnets and the ages of the Alpine high-pressure metamorphism [Dataset]. Nature, *387*, 586–589. https://doi.org/10.1038/42446

Elhlou, S., Belousova, E., Griffin, W. L., Pearson, N. J., & O'reilly, S. Y. (2006). Trace element and isotopic composition of GJ-red zircon reference material by laser ablation [Dataset]. Geochimica et Cosmochimica Acta, *70*, A158. https://doi.org/10.1016/j.gca.2006.06.1383

Faure, G., & Mensing, T. (2005). Isotopes: Principles and Applications Chapter 12. In *The Lu-Hf method*. (3rd ed., pp. 284–296). John Wiley and Sons, INC.

Gerdes, A., & Zeh, A. (2009). Zircon formation versus zircon alteration—New insights from combined U-Pb and Lu-Hf in-situ LA-ICP-MS analyses, and consequences for the interpretation of Archean zircon from the Central zone of the Limpopo belt [Dataset]. Chemical Geology, *261*, 230–243. https://doi.org/10.1016/j.chemgeo.2008.03.005

Griffin, W. L., Pearson, N. J., Belousova, E., Jackson, S. E., O'reilly, S. Y., Van Achterberg, E., & Shee, S. R. (2000). The Hf isotope composition of cratonic mantle: LAM-MC-ICPMS analysis of zircon megacrysts in kimberlites [Dataset]. Geochimica et Cosmochimica Acta, *64*, 133–147. https://doi.org/10.1016/S0016-7037(99)00343-9

Griffin, W. L., Belousova, E. A., Walters, S. G., & O'Reilly, S. Y. (2006). Archaean and Proterozoic crustal evolution in the eastern Succession of the Mt Isa district, Australia: U–Pb and Hf-isotope studies of detrital zircons [Dataset]. Australian Journal of Earth Sciences, *53*, 125–149. https://doi.org/10.1080/08120090500434591

Hawkesworth, C. J., & Kemp, A. (2006). Using hafnium and oxygen isotopes in zircons to unravel the record of crustal evolution [Dataset]. Chemical Geology, *226*(3–4), 144–162. https://doi.org/10.1016/j.chemgeo.2005.09.018

Jackson, S. E., Pearson, N. J., Griffin, W. L., & Belousova, E. (2004). The application of laser ablation inductively coupled plasma mass spectrometry to in-situ U–Pb zircon geochronology [Dataset]. Chemical Geology, *211*(1–2), 47–69. https://doi.org/10.1016/j.chemgeo.2004.06.017

López de Luchi, M. L., Hoffmann, A., Siegesmund, S., Wemmer, K., & Steenken, A. (2002). Temporal constraints on the polyphase evolution of the Sierra de San Luis. Preliminary report based on biotite and muscovite cooling ages. In *Actas 15 Congreso Geológico Argentino (Proceedings of 15th Argentine Geological Congress)*. (Vol. 1, pp. 309–315).

Ludwing, K. R. (2003). Isoplot 3.00: A Geochronological tool kit for Microsoft Excel. *Berkeley Geochrnological Center, Special Publications*.

Morel, M. L. A., Nebel, O., Nebel-Jacobsen, Y. J., Miller, J. S., & Vroon, P. Z. (2008). Hafnium isotope characterization of the GJ-1 zircon reference material by solution and laser-ablation MC-ICPMS [Dataset]. Chemical Geology, *255*(1–2), 231–235. https://doi.org/10.1016/j.chemgeo.2008.06.040

Patchett, P. J., & Tatsumoto, M. (1980). Hafnium isotope variations in oceanic basalts [Dataset]. Geophysical Research Letters, *7*, 1077–1080. https://doi.org/10.1029/GL007i012p01077

Patchett, P. J., & Tatsumoto, M. (1981). Lu/Hf in chondrites and definition of a chondritic hafnium growth curve [Dataset]. Lunar and Planetary Science, *12*, 822. Retrieved fromhttps://adsabs.harvard.edu/full/1981LPI....12..822P

Patchett, P. J., Kouvo, O., Hedge, C. E., & Tatsumoto, M. (1981). Evolution of continental crust and mantle heterogeneity: Evidence from Hf isotopes [Dataset]. Contributions to Mineralogy and Petrology, *78*, 279–297. https://doi.org/10.1007/BF00398923

Schmidt, A., Weyer, S., Mezger, S., Scherer, E., Xiao, Y., Hoefs, J., & Brey, J. (2008). Rapid eclogitisation of the Dabie–Sulu UHP terrane: Constraints from Lu–Hf garnet geochronology [Dataset]. Earth and Planetary Science Letters, *273*(1–2), 203–213. https://doi.org/10.1016/j.epsl.2008.06.036

Sato, A. M., González, P. D., Petronilho, L. A., Llambías, E. J., Varela, R., & Basei, M. A. S. (2001). Sm-Nd, Rb-Sr and K-Ar age constraints of the El Molle and Barroso plutons, western Sierra de San Luis, Argentina. 3° South American symposium on isotope geology, extended abstract volume (CD). *Sociedad Geológica de Chile*, 241–244.

Sato, A. M., González, P. D., Basei, M. A., Passarelli, C. R., Tickyj, H., & Ponce, J. M. (2003). The famatinian granitoids of southwestern Sierra de San Luis, Argentina. In *IV South American Symposium on Isotope Geology* (pp. 290–293).

Silva Nieto, D. G., Márquez, M. J., Ardolino, A. A., & Franchi, M. (2005). Hoja Geológica 4369-III Paso de Indios. Provincia del Chubut [Dataset]. Instituto de Geología y Recursos Minerales, Servicio Geológico Minero Argentino. Boletín, *267*, 64.https://repositorio.segemar.gov.ar/handle/308849217/165

Sims, J. P., Ireland, T. R., Camacho, A., Lyons, P., Pieters, P. E., Skirrow, R. G., et al. (1998). U-Pb, Th-Pb and Ar-Ar geochronology from the southern Sierras Pampeanas, Argentina: Implications for the Palaeozoic tectonic evolution of the western Gondwana margin [Dataset]. Geological Society, London, Special Publications, *142*, 259–281. https://doi.org/10.1144/GSL.SP.1998.142.01.13

Steenken, A., López de Luchi, M. G., Siegesmund, S., Wemmer, K., & Pawlig, S. (2004). Crustal provenance and cooling of the basement complexes of the Sierra de San Luis: An insight into the tectonic history of the proto-Andean margin of Gondwana [Dataset]. Gondwana Research, *7*, 1171–1195. https://doi.org/10.1016/S1342-937X(05)71092-3

Steenken, A., Siegesmund, S., Wemmer, K., & López de Luchi, M. G. (2008). Time constraints on the famatinian and Achalian structural evolution of the basement of the Sierra de San Luis (eastern Sierras Pampeanas, Argentina) [Dataset]. Journal of South American Earth Sciences, *25*, 336–358. https://doi.org/10.1016/j.jsames.2007.05.002

Steiger, R. H., & Jäger, E. (1977). Subcommission on geochronology: Convention on the use of decay constants in geo-and cosmochronology [Dataset]. Earth and Planetary Science Letters, *36*, 359–362. https://doi.org/10.1016/0012-821X(77)90060-7

Tickyj, H., Cingolani, C., Varela, R., & Chemale, F., Jr. (2001). Rb-Sr ages from La Horqueta formation, San Rafael block, Argentina. In *South American symposium on isotope geology* (pp. 628–631).

Toubes, R. O., & Spikermann, J. P. (1976). Algunas edades KAr para la Sierra Pintada, provincia de Mendoza. *Revista de la Asociación Geológica Argentina*, *31*, 118–126.

Vervoort, J. D., & Blichert-Toft, J. (1999). Evolution of the depleted mantle: Hf isotope evidence from juvenile rocks through time [Dataset]. Geochimica et Cosmochimica Acta, *63*(3–4), 533–556. https://doi.org/10.1016/S0016-7037(98)00274-9

Vervoort, J. (2014). Lu-Hf dating: The Lu-Hf isotope System. [Dataset]. Encyclopedia of Scientific dating methods. In W. Rink, & J. Thompson (Eds.), Springer. https://doi.org/10.1007/978-94-007-6326-5_46-1

Vervoort, J. D., & Kemp, A. I. S. (2016). Clarifying the zircon Hf isotope record of crust -mantle evolution [Dataset]. Chemical Geology, *425*, 65–75. https://doi.org/10.1016/j.chemgeo.2016.01.023

Woodhead, J., Hergt, J., Shelley, M., Eggins, S., & Kemp, R. (2004). Zircon Hf-isotope analysis with an excimer laser, depth profiling, ablation of complex geometries and concomitant age estimation [Dataset]. Chemical Geology, *209*, 121–135. https://doi.org/10.1016/j.chemgeo.2004.04.026

Woodhead, J. D., & Hergt, J. M. (2005). A preliminary appraisal of seven natural zircon reference materials for in situ Hf isotope determination [Dataset]. Geostandards and Geoanalytical Research, *29*, 183–195. https://doi.org/10.1111/j.1751-908X.2005.tb00891.x

Zeh, A., Gerdes, A., Klemd, R., & Barton, J., Jr. (2007). Archaean to Proterozoic crustal evolution in the central zone of the Limpopo belt (South Africa-Botswana): Constraints from Combined U-Pb and Lu-Hf isotope Analyses of zircon [Dataset]. Journal of Petrology, *48*, 1605–1639. https://doi.org/10.1093/petrology/egm032